

Theory of Tunneling Anomaly in Superconductor above Paramagnetic Limit

Hae-Young Kee¹, I.L. Aleiner^{2,3}, and B.L. Altshuler^{2,4}

¹*Serin Physics Laboratory, Rutgers University, Piscataway, NJ 08855*

²*NEC Research Institute, 4 Independence Way, Princeton, NJ 08540*

³*Department of Physics and Astronomy, SUNY at Stony Brook, Stony Brook, NY 11794*

⁴*Physics Department, Princeton University, Princeton, NJ 08544*

We study the tunneling density of states (DoS) in the superconducting systems driven by Zeeman splitting E_Z into the paramagnetic phase. We show that, even though the BCS gap disappears, superconducting fluctuations cause a strong DoS singularity in the vicinity of energies $-E^*$ for electrons polarized along the magnetic field and E^* for the opposite polarization. The position of this singularity $E^* = \frac{1}{2} \left(E_Z + \sqrt{E_Z^2 - \Delta^2} \right)$ (where Δ is BCS gap at $E_Z = 0$) is universal. We found analytically the shape of the DoS for different dimensionality of the system. For ultra-small grains the singularity has the shape of the hard gap, while in higher dimensions it appears as a significant though finite dip. The spin-orbit scattering, and the orbital magnetic field suppress the singularity. Our results are qualitatively consistent with recent experiments in superconducting films.

PACS numbers: 74.40.+k, 74.50.+r, 73.40Gk, 73.50.-h

I. INTRODUCTION

It is well known that the magnetic field, H , suppresses superconductivity since it lifts time reversal symmetry (see *e.g.* Ref. 1 for general introduction). In the absence of the spin orbit coupling, this effect can be separated into two mechanisms: (i) effect of the magnetic field on the orbital motion associated with Aharonov-Bohm phase, and (ii) Zeeman splitting of the states with the same spatial wave functions but opposite spin directions.

In the bulk systems, the suppression of the superconductivity is typically associated with the first mechanism. Indeed, the estimate for the critical field H_{c2} in this case is

$$H_{c2} \xi^2 \simeq \phi_0, \quad (1.1)$$

where $\phi_0 = \frac{hc}{2e}$ is the superconducting flux quantum and

$$\xi = \sqrt{\frac{D}{\Delta}} \quad (1.2)$$

is the coherence length for the dirty superconductors, Δ is the BCS gap, and D is the diffusion coefficient. On the other hand, the magnetic field necessary to affect the superconductivity by virtue of the spin mechanism is given by

$$g_L \mu_B H_{spin} \simeq \Delta, \quad (1.3)$$

where g_L is the Landé g -factor, and $\mu_B = \frac{e\hbar}{2mc}$ is the Bohr magneton. Comparing Eqs. (1.1) and (1.3), one finds that H_{spin} is far in excess of H_{c2} :

$$\frac{H_{spin}}{H_{c2}} \simeq \epsilon_F \tau \gg 1, \quad (1.4)$$

where ϵ_F is the Fermi energy and τ is the elastic momentum relaxation time. Condition (1.4) means that in the bulk system, the orbital effect of the magnetic field is always dominant.

Situation may change in the restricted geometries. Consider, *e.g.*, the superconducting film of the thickness $a \ll \xi$, placed in the magnetic field parallel to the plane of the film. The Cooper pair in this case is restricted in the transverse direction by the film thickness a . As a result, the geometrical area swept by this pair can be estimated as $a\xi$ rather than as ξ^2 . Therefore, Eq. (1.1) should be changed to

$$H_{c2}^{\parallel} \xi a \simeq \phi_0 \quad \Rightarrow \quad H_{c2}^{\parallel} \simeq H_{c2} \left(\frac{\xi}{a} \right). \quad (1.5)$$

On the other hand, Zeeman splitting $E_Z = g_L \mu_B H$ is not affected by geometrical restriction. Accordingly, instead of Eq. (1.4) the ratio of the two scales of magnetic field is given by

$$\frac{H_{spin}}{H_{c2}^{\parallel}} \simeq (\epsilon_F \tau) \left(\frac{a}{\xi} \right). \quad (1.6)$$

Thus, for sufficiently thin films, $a \ll \frac{\xi}{\epsilon_F \tau}$, the spin effects become dominant. One can easily check that the same estimate (1.6) holds for other restricted systems, i.e., superconducting grains or wires. In these cases, a is the size of the grain or the diameter of the wire respectively. Quite generally, a is determined by the minimal size of the sample in the plane perpendicular to the magnetic field. In this paper we consider such restricted geometries, and unless the opposite is stated, neglect the orbital effects.

The transition from superconductor to paramagnet is of the first order²: superconducting state is the only stable state at $E_Z \leq \Delta$; while at $E_Z \geq 2\Delta$ normal state is the only stable state. Both phases are locally stable in the interval of magnetic fields where $\Delta < E_Z < 2\Delta$. The normal state becomes lowest in energy and thus globally stable at $E_Z \geq \sqrt{2}\Delta$. From now on, we will assume that this condition is fulfilled.

One of the most fundamental manifestations of the superconductivity is the gap in the tunneling density of states (DoS) around the zero bias^{1,3}. One can expect that after the paramagnetic transition not only BCS order parameter vanishes but also the energy dependence of tunneling DoS becomes similar to those in superconductors above critical temperature T_c . (The latter dependence is discussed in the review article Ref. 4.)

In this paper, we demonstrate that, on the contrary, there are clear observable superconducting effects in the normal state even far from the transition region. We will show that at the transition point there appears a dip in the DoS (schematic evaluation of the DoS with the magnetic field is shown in Fig. 1).

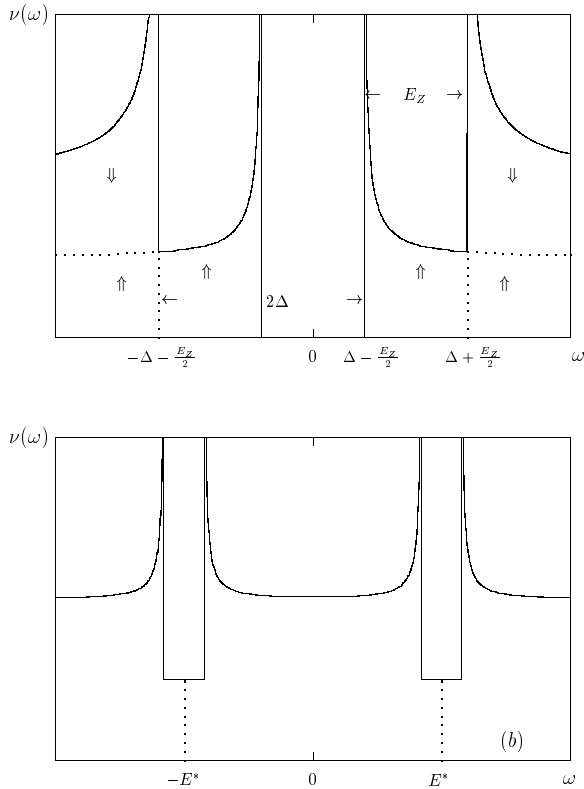


FIG. 1. Evolution of the tunneling DoS with the Zeeman splitting E_Z for (a) the superconducting state, $E_Z < \sqrt{2}\Delta$, see *e.g.* Ref. 5, and (b) for the paramagnetic state $E_Z > \sqrt{2}\Delta$. The usual zero bias anomaly in the paramagnetic state (b) is not shown for simplicity. Shape of the singularity at E^* corresponds to the 0-dimensional case.

The shape and the width of this dip depend on dimensionality of the system. However, its position is remarkably universal:

$$E^* = \frac{1}{2}(E_Z + \sqrt{E_Z^2 - \Delta^2}), \quad (1.7)$$

for 0D (grain), 1D (strip), and 2D (film) cases. Some of conclusions have been already briefly reported by two of us⁶. Here we present detailed derivations of results of Ref. 6 and consider the relevant perturbations (spin-orbital coupling, orbital magnetic field, finite temperature, and energy relaxation) of the new tunneling anomaly.

The remainder of the paper is organized as follows. Section II presents the parametrically exact solution for the simplest but instructive geometry of zero-dimensional systems (ultra-small superconducting grains). Section III deals with more involved problem of the tunneling anomaly in the superconducting films and wires. Both sections required application of the diagrammatic technique on the level of at least Ref. 7. For the benefit of the readers interested in physical interpretation rather than in rigorous derivations, we present in Sec. IV the qualitative derivation which grasps all the essential physics involved, even though fails to give the completely quantitative description. Section V analyzes how the tunneling anomaly is affected by spin-orbital coupling, orbital magnetic field, finite temperature, and energy relaxation. We discuss the recent experiment⁸ on the Zeeman splitting of the tunneling anomaly in Al films in Sec. VI. Our findings are summarized in Conclusion.

II. ZERO DIMENSIONAL SYSTEMS

Let us consider an isolated disordered superconducting grain which is small so that the Zeeman splitting dominates over the orbital magnetic field effect (see, *e.g.*, Refs. 9,10 for recent experiments on such grains). We assume that the size of the grain exceeds electronic mean free path l , and, at the same time, it is much smaller than the superconducting coherence length ξ . We also assume that $k_F l \gg 1$. This results in the large dimensionless conductance of the grain g ($g \sim k_F^2 l a$). Finally, we assume that the grain is already driven into the paramagnetic state by the Zeeman splitting. Our goal is to find effects of the superconducting fluctuations on the DoS of the system.

The Hamiltonian H of the system consists of noninteracting part H_0 and interacting one H_{int} . Using the basis of the exact eigenstates of H_0 labeled by integers i and j , one can write the Hamiltonian as

$$H = \sum_{i\sigma} E_{i\sigma} a_{i\sigma}^\dagger a_{i\sigma} - \lambda \bar{\delta} \sum_{i,j} a_{i\uparrow}^\dagger a_{i\downarrow}^\dagger a_{j\downarrow} a_{j\uparrow}. \quad (2.1)$$

Here operator $a_{i\sigma}^\dagger$ ($a_{i\sigma}$) creates(annihilates) an electron in a state i with spin $\sigma = \uparrow, \downarrow$, and energy $E_{i\uparrow(\downarrow)} = \epsilon_i \mp E_Z/2$ where ϵ_i is the orbital energy of i -th state. $\lambda \ll 1$ is the dimensionless interaction constant, and $\bar{\delta}$ is the average level spacing:

$$\langle \epsilon_{i+1} - \epsilon_i \rangle = \bar{\delta}. \quad (2.2)$$

Let us stop for a moment to discuss the approximation made in Eq. (2.1). We included in Eq. (2.1) only the matrix elements of the interaction Hamiltonian responsible for the superconductivity. We omitted two kinds of diagonal terms. The term proportional to $a_{i\sigma_1}^\dagger a_{i\sigma_1} a_{j\sigma_2}^\dagger a_{j\sigma_2}$ represents the total charging energy responsible for the Coulomb blockade¹¹. It is not important for us because it does not lead to any anomalies at energies of the order of Zeeman splitting, and it can be accounted for by the corresponding shift of the applied bias. Other diagonal terms such as the one proportional to $a_{i\sigma_1}^\dagger a_{i\sigma_2} a_{j\sigma_2}^\dagger a_{j\sigma_1}$ represents the spin exchange. It is not included because it leads only to the renormalization of the Landé factor g_L .

We also omitted off-diagonal terms, such as $a_{i\uparrow}^\dagger a_{j\downarrow}^\dagger a_{k\downarrow} a_{l\uparrow}$ with i, j, k, l not equal pairwise, corresponding to the matrix elements:

$$M_{ij}^{kl} = \int dr dr' V(r - r') \psi_i^*(r) \psi_j^*(r') \psi_k(r) \psi_l(r').$$

The wave functions are known to oscillate very fast, so the wavefunctions of different levels are very weakly correlated. We can restrict our consideration by short range interaction, $V(r - r') = \frac{\lambda}{\nu_0} \delta(r - r')$, where ν_0 is the bare DoS. One see that the integrand ($|\psi_i(r)|^2 |\psi_j(r)|^2$) in the diagonal matrix elements is always positive while the product ($\psi_i^*(r) \psi_j^*(r) \psi_k(r) \psi_l(r)$) can be both positive and negative. As a result, the off-diagonal matrix elements turn out to be smaller than diagonal ones. Straightforward calculation^{12,13} shows that they are smaller by the factor $1/g$.

In the paramagnetic state ($E_Z > \sqrt{2}\Delta$), the structure of the ground state is similar to that without interaction, see Fig. 2. The orbitals with $\epsilon_i < -E_Z/2$ are doubly occupied while those with $\epsilon_i > E_Z/2$ are empty. The orbitals with $|\epsilon_i| < E_Z/2$ are spin-polarized with up-spin.

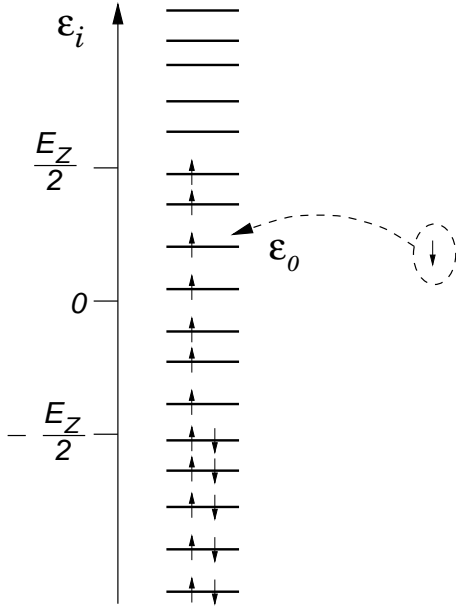


FIG. 2. Structure of the ground state of the superconductor above paramagnetic limit. Electron tunneling onto the orbital ϵ_0 , creates the spin single states on this orbital. At some energy ϵ_0 mixing of this singlet with the empty states becomes resonant, see the text.

The Hamiltonian (2.1) does not affect the spin polarized states, but mixes the doubly-occupied and empty states. Since those states are separated from each other by a large gap E_Z , this mixing can be treated perturbatively. Thus, the mixing does not change the ground state qualitatively. On the contrary, the spectrum of the excitations, i.e., the tunneling DoS changes drastically due to the interaction. The essence of this effect is that spin-down electron tunneling into some orbital ϵ_0 already occupied by spin down electron creates an electron pair which can mix with the empty orbitals and thus interact with superconducting fluctuations. This mixing turns out to be resonant at some energy $E = E^*$ and it leads to the sharp singularity in the spectrum of one-electron excitation.

To evaluate the effect of superconducting fluctuations on the DoS of electrons in the paramagnetic state, we use the diagrammatic technique for the Green function (GF) at zero-temperature⁷. The DoS can be expressed through the one particle GF, $G_{i\sigma}(\omega)$, of an electron on the orbital j and with spin $\sigma = \pm 1 \equiv \uparrow (\downarrow)$:

$$\nu_\sigma(\omega) = -\frac{1}{\pi} \text{sgn}(\omega) \text{Im} \sum_i G_{i\sigma}(\omega), \quad (2.3)$$

where

$$G_{i\sigma}^{-1} = G_{i\sigma}^{0-1} - \Sigma_{i\sigma}. \quad (2.4)$$

$G_{i\sigma}^0$ is the GF for the non-interacting system

$$G_{i\uparrow(\downarrow)}^0 = (\omega_+ - \epsilon_i \pm E_Z/2)^{-1}, \quad (2.5)$$

and $\Sigma_{i\sigma}$ is the one particle self-energy.

Leading contribution to the self-energy is shown in Fig. 3a. The solid and curly lines denote single-particle GF and the propagator of superconducting fluctuations, respectively. The latter can be obtained by summing the polarization loops in the Cooper channel shown in Fig. 3b. The single loop is given by

$$\Pi(\omega) = \frac{1}{2\delta} \ln \left(\frac{\omega_c^2}{E_Z^2 - \omega_+^2} \right), \quad (2.6)$$

where $\omega_+ = \omega + i0 \text{sgn}(\omega)$ and ω_c is the high-energy cut-off. Solving the Dyson equation (Fig. 3b), we obtain the propagator

$$\Lambda(\omega) = \frac{\lambda\bar{\delta}}{1 - \lambda\bar{\delta}\Pi(\omega)} = \frac{2\bar{\delta}}{\ln\left(\frac{E_Z^2 - \omega^2}{\Delta^2}\right)}, \quad (2.7)$$

where $\Delta = \omega_c \exp(-1/\lambda)$ is the BCS gap.

The propagator (2.7) has the pole at $\omega = \pm\Omega$,

$$\Omega = \sqrt{E_Z^2 - \Delta^2}. \quad (2.8)$$

This pole can be interpreted as the bound state of two quasiparticles with energy Ω .

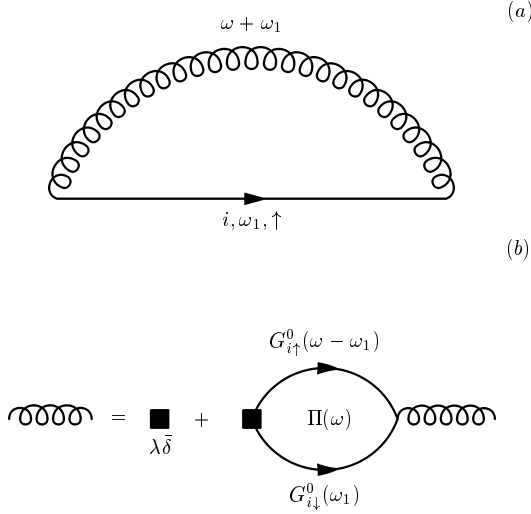


FIG. 3. Diagrams for (a) self-energy $\Sigma_{i,\downarrow}(\omega)$ and (b) superconducting propagator $\Lambda(\omega)$.

Analytic expression for the self-energy given by diagram Fig. 3a, has the form

$$\Sigma_{i\downarrow}(\omega) = i \int_{-\infty}^{\infty} \frac{d\omega_1}{2\pi} \Lambda(\omega + \omega_1) G_{i\uparrow}^0(\omega_1). \quad (2.9)$$

One can see that there are two contributions to the self-energy. One comes from the pole of Λ and the other is due to the branch-cut of this propagator. The pole contribution gives a singularity of the self-energy at certain ω and ϵ_i while the contribution of the branch-cut is smooth. To find the singularity in the DoS, only the pole contribution to Σ may be retained:

$$\Sigma_{i\downarrow}(\omega) = \frac{\bar{\delta}\Delta^2}{\Omega} \frac{1}{\omega_+ + \epsilon_i - E_Z/2 + \Omega \text{sgn}(\epsilon_i - E_Z/2)}. \quad (2.10)$$

At certain ω the pole of the self-energy coincides with the pole of G^0 . This causes the singularity in the DoS. One can check that singularities of Eq. (2.5) and Eq. (2.10) coincide provided $\epsilon_i = \Omega/2$ and

$$\omega = \frac{E_Z + \Omega}{2} = \frac{E_Z + \sqrt{E_Z^2 - \Delta^2}}{2} \equiv E^*. \quad (2.11)$$

Substituting Eq. (2.10) into Eq. (2.4) we obtain the GF for the down-spin electron at ω close to E^* :

$$G_{i\downarrow}(\omega) = \frac{\omega_+ + \epsilon_i - E_Z/2 - \Omega}{(\omega_+ - \epsilon_i - E_Z/2)(\omega_+ + \epsilon_i - E_Z/2 - \Omega) - W_0^2}, \quad (2.12)$$

where energy scale of the singularity is given by

$$W_0 = \sqrt{\frac{\bar{\delta}\Delta^2}{\Omega}}. \quad (2.13)$$

Since $E_Z, \Delta \gg \bar{\delta}$, one can neglect the fine structure of the DoS on the scale of $\bar{\delta}$ and substitute the summation over i by the integration over ϵ_i :

$$\begin{aligned} \sum_i G_{i\downarrow} &= \nu_0 \int d\epsilon_i \frac{\omega_+ + \epsilon_i - E_Z/2 - \Omega/2}{-\epsilon_i^2 + (\omega_+ - E_Z/2 - \Omega/2) - W_0^2} \\ &= -i\nu_0\pi \frac{\omega - E^*}{\sqrt{(\omega - E^*)^2 - W_0^2}}. \end{aligned} \quad (2.14)$$

Analogously, the GF for the up-spin electron can be obtained by changing the signs of E_Z and Ω , so that the singularity occurs at $\omega = -E^*$.

Substituting Eq. (2.14) into Eq. (2.3), we obtain the final expression for the tunneling DoS in the ultra-small grains

$$\nu_{\uparrow(\downarrow)}(\omega) = \nu_0 F_0 \left(\frac{\omega \pm E^*}{W_0} \right), \quad F_0(x) = \text{Re} \left(\frac{x^2}{x^2 - 1} \right)^{1/2}, \quad (2.15)$$

where ν_0 is the bare DoS per one spin, energy E^* is defined by Eq. (1.7) and width of the singularity W_0 is given by Eq. (2.13). Equations (2.15) and (2.13) are the main result of this section. They predict the hard gap in the spin resolved density of states: $\nu_\sigma(\omega)$ vanishes at $|\omega + \sigma E^*| < W_0$. Overall density of states $\nu_\downarrow + \nu_\uparrow$ is suppressed by a factor of two near the singularity.

In this calculation we neglected higher corrections to the self energy, *e.g.*, those shown in Fig. 4a, b. In order to justify this approximation, we have to compare contributions shown in Figs. 4a, b with the reducible diagram shown in Fig. 4c included in Eqs. (2.10) and (2.12). Singular contribution originates from the pole of Λ . It means that Λ carries frequency Ω . The singularity in the DoS at $\omega = E^*$ appears when the pole of the self-energy and the pole of G^0 coincide. This happens when GF G^0 for up-spin carries energy $\Omega - \omega$. In diagrams Fig. 4a, b, and c, the intermediate G^0 for down-spin should carry energy ω to give singularity to the DoS at E^* . This condition can not be satisfied for the diagrams Fig. 4a, b. As a result, after the integration over the intermediate frequency, these higher order corrections turns out to be smaller than the reducible contribution (c) by small factor $W_0/\Delta \simeq \sqrt{\bar{\delta}/\Delta} \ll 1$.

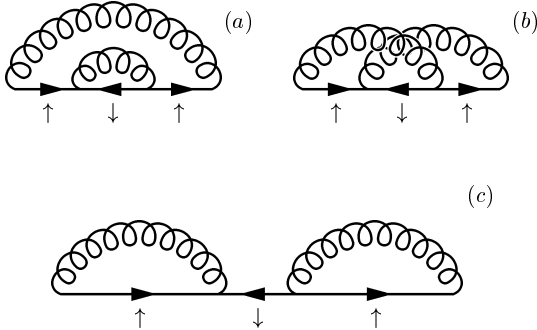


FIG. 4. Higher order correction to the self-energy (a) and (b), which were neglected in comparison with reducible diagram (c).

III. DISORDERED INFINITE SYSTEMS

In this section, we will obtain the quantitative results for the tunneling anomaly in the infinite systems. In subsection III A we will start from the perturbation theory and demonstrate that the lowest order perturbative results diverge algebraically at energies close to E^* . In order to deal with this divergence, we develop non-perturbative approach in subsection III B and obtain the analytic expressions for the shape of the singularities for all interesting cases. This machinery will be also used later in Sec. V.

A. Perturbative results

The analysis of 0-D system presented in the previous subsection, is not directly applicable to superconducting wires and films because one can not approximate interaction Hamiltonian

$$\hat{H}_{int} = -\lambda\nu_0^{-1} \int_{-\infty}^{\infty} dr a_{\uparrow}^{\dagger}(r)a_{\downarrow}^{\dagger}(r)a_{\downarrow}(r)a_{\uparrow}(r). \quad (3.1)$$

by its diagonal matrix elements. Despite this complication, we will still be able to show that the singularity persists and remains at the same bias as that in 0-D.

To describe this singularity we once again have to evaluate the effect of the superconducting fluctuations on the GF of electrons. First of all, we need to evaluate the propagator of superconducting fluctuations Λ , see Fig. 5. In contrast with 0-D case, the superconducting fluctuations in the bulk system are inhomogeneous: the propagator for the superconducting fluctuations depends on the wave vector Q . (We will omit the vector notation in the momenta, e.g., $Q \equiv \vec{Q}$.) Solving the Dyson equation, shown in Fig. 5a, we obtain the propagator

$$\Lambda(\omega, Q) = \frac{2}{\nu_0 \ln \left(\frac{E_Z^2 - (|\omega| + iDQ^2)^2}{\Delta^2} \right)}, \quad (3.2)$$

where D is the diffusion coefficient. At $Q = 0$, propagator (3.2) resembles zero-dimensional expression (2.7). We see that the propagator has the singularity at ω close to Ω provided $DQ^2 \ll \Omega$. As we will see shortly, it results in the singularity in the DoS developing at exactly the same energy as in 0-D case, $\omega = E^*$, given by Eq. (2.11).

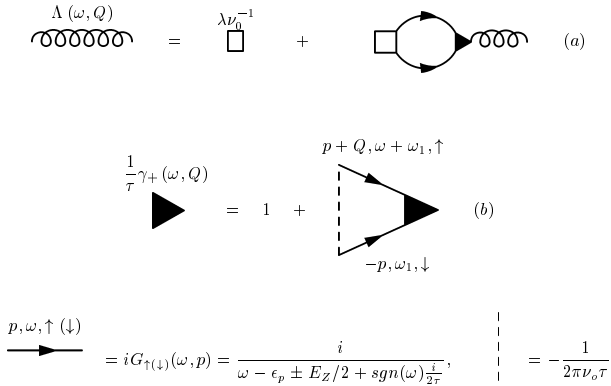


FIG. 5. Diagrams for the (a) propagator of superconducting fluctuations $\Lambda(\omega, Q)$ and (b) the vertex function $\gamma_+(\omega, Q)$.

Next step is to consider vertex function in the particle-particle channel. The ladder approximation which gives the main contribution at $\epsilon_F\tau \gg 1$ (τ is the elastic mean free time) is shown in Fig. 5b. Analytically, they are given by

$$\gamma_{\pm}(\omega, Q) = \tau + I_{\pm}(\omega, Q)\gamma_{\pm}(\omega, Q). \quad (3.3)$$

Here $I_{\pm}(\omega, Q)$ stands for

$$\begin{aligned} I_{\pm}(\omega, Q) &= \frac{1}{2\pi\nu_0\tau} \int (dp) G_{\uparrow(\downarrow)}(\omega + \omega_1, \epsilon_p) G_{\downarrow(\uparrow)}(\omega_1, \epsilon_{-p-Q}) \\ &= \frac{1}{2\pi\nu_0\tau} \int (dp) \frac{1}{(\omega + \omega_1 - \epsilon_p \pm \frac{E_Z}{2} + \frac{i}{2\tau} \text{sgn}(\omega + \omega_1))(\omega_1 - \epsilon_{-p+Q} \mp \frac{E_Z}{2} + \frac{i}{2\tau} \text{sgn}(\omega_1))} \\ &= \{1 + \tau [i(|\omega| \pm \text{sgn}(\omega)E_Z) - DQ^2]\} \theta[-(\omega + \omega_1)\omega], \end{aligned} \quad (3.4)$$

where $(dp) = \frac{d^d p}{(2\pi)^d}$, and the GFs are averaged over disorder^{7,4}. Here we used the conditions of the diffusion approximation, $\omega\tau \ll 1$ and $Ql \ll 1$. We substitute Eq. (3.4) into Eq. (3.3) and we obtain

$$\gamma_{\pm}(\omega, Q) = \tau\theta[(\omega + \omega_1)\omega] + \frac{\theta[-(\omega + \omega_1)\omega]}{-i[|\omega| \pm \text{sgn}(\omega)E_Z] + DQ^2}. \quad (3.5)$$

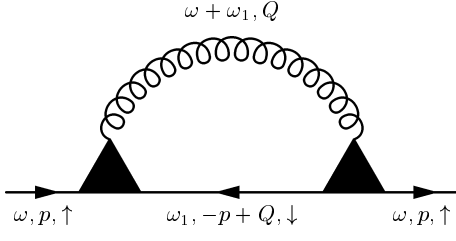


FIG. 6. Diagrams for the lowest order corrections to the one-particle Green function.

Now we can evaluate the first order correction to the one-particle GF, Fig. 6:

$$\delta G_{\downarrow}^{(1)}(\omega, p) = \frac{1}{\tau^2} \int (dQ) \int \frac{d\omega_1}{2\pi} G_{\downarrow}^2(\omega, p) \Lambda(\omega + \omega_1, Q) G_{\uparrow}(\omega_1, -p + Q) \gamma_-^2(\omega - \omega_1, Q) \quad (3.6)$$

The DoS is determined by the GF integrated over p :

$$\nu_{\uparrow(\downarrow)}(\omega) = -\frac{\text{sgn}(\omega)}{\pi} \text{Im} \int (dp) G_{\uparrow(\downarrow)}(\omega, p) \quad (3.7)$$

We substitute Eq. (3.5) into Eq. (3.7) and perform the integration over p and ω_1 . For $Ql \ll 1$ and $|\omega - \omega_1|\tau \ll 1$ integration over the momentum p results in

$$\int (dp) G_{\downarrow}^2(\omega, p) G_{\uparrow}(\omega_1, -p + Q) = i2\pi\nu_0\theta(-\omega\omega_1)\tau^2 \text{sgn}(\omega_1).$$

Performing integration over ω_1 we take into account only the pole contributions in the propagator (3.2) for $DQ^2 \ll \Omega$:

$$\Lambda(\omega, Q) \approx \frac{\Delta^2}{\nu_0\Omega} \left(\frac{1}{\Omega + \omega - iDQ^2} + \frac{1}{\Omega - \omega - iDQ^2} \right). \quad (3.8)$$

since the integrals along the branch cuts give only the corrections which are smooth functions of ω . The main contribution to the frequency integral results from the region where the real part of the pole of the propagator Λ in Eq. (3.7), $\text{Re } \omega_1 = -\omega \pm \Omega$ is close to that of the vertex γ_- , $\text{Re } \omega_1 = \omega + \text{sgn}(\omega_1 - \omega)E_Z$, and the imaginary parts of those poles have different signs. The latter requires $\omega \text{Re } \omega_1 < 0$, $\omega^2 > [\text{Re } \omega_1]^2$. One can easily check that all these conditions can be met only if ω is close to E^* from Eq. (1.7).

Evaluating the integral over ω_1 in Eq. (3.7) we obtain the first order correction to the DoS

$$\frac{\delta\nu_{\uparrow(\downarrow)}^{(1)}(\omega)}{\nu_0} = -\frac{\Delta^2}{2\nu_0\Omega} \text{Re} \int (dQ) C^2(\omega \pm E^*, Q), \quad (3.9)$$

where $C_{\uparrow(\downarrow)}(\omega, Q)$ is the Cooperon given by

$$C(\omega, Q) = \frac{1}{-i|\omega| + DQ^2}. \quad (3.10)$$

[Calculation of $\delta\nu_{\uparrow}$ requires an obvious modification of Eq. (3.7).]

For one dimensional case (wire), this correction acquires the form

$$\frac{\delta\nu_{\uparrow(\downarrow)}^{(1)}(\omega)}{\nu_0} = \frac{\sqrt{\Delta}}{8\nu_0\Omega\sqrt{2D}} \left(\frac{\Delta}{|\omega \pm E^*|} \right)^{3/2}. \quad (3.11)$$

It is possible to neglect higher order corrections to DoS only provided $|\omega \pm E^*|$ is large. For $\omega \rightarrow E^*$, correction (3.11) diverges. Therefore we need to sum up all the orders of perturbation theory to describe the DoS in the vicinity of E^* . Such calculation is carried out in the next subsection.

For two dimensions (films), the first order correction to the DoS vanishes for $|\omega| \neq E^*$. However, this is nothing but an artifact of the first order approximation and the second order correction is already finite. Diagrams for this correction are shown in Fig. 7. The result can be written as:

$$\frac{\delta\nu^{(2)}(\omega)_{\uparrow(\downarrow)}}{\nu_0} = -2 \left(\frac{\Delta^2}{4\nu_0\Omega} \right)^2 \frac{\partial}{\partial\omega} \text{Im} \int (dQ_1)(dQ_2) C_{\uparrow(\downarrow)}^2(\omega, Q_1) C_{\uparrow(\downarrow)}(\omega, Q_2). \quad (3.12)$$

For two dimensional case Eq. (3.12) gives

$$\frac{\delta\nu_{\uparrow(\downarrow)}^{(2)}(\omega)}{\nu_0} = - \left[\frac{\Delta^2}{4g\Omega(\omega \pm E^*)} \right]^2 \ln \left(\frac{\Omega}{|\omega \pm E^*|} \right)^2, \quad (3.13)$$

where $g = 4\pi D\nu_0 \gg 1$ is the dimensionless conductance of the film in the normal state. Deriving Eq. (3.13), we cut off the logarithmic divergence at large momenta Q_2 by the condition $DQ_2^2 \lesssim \Delta$, since it determines the applicability of a single pole approximation (3.8).

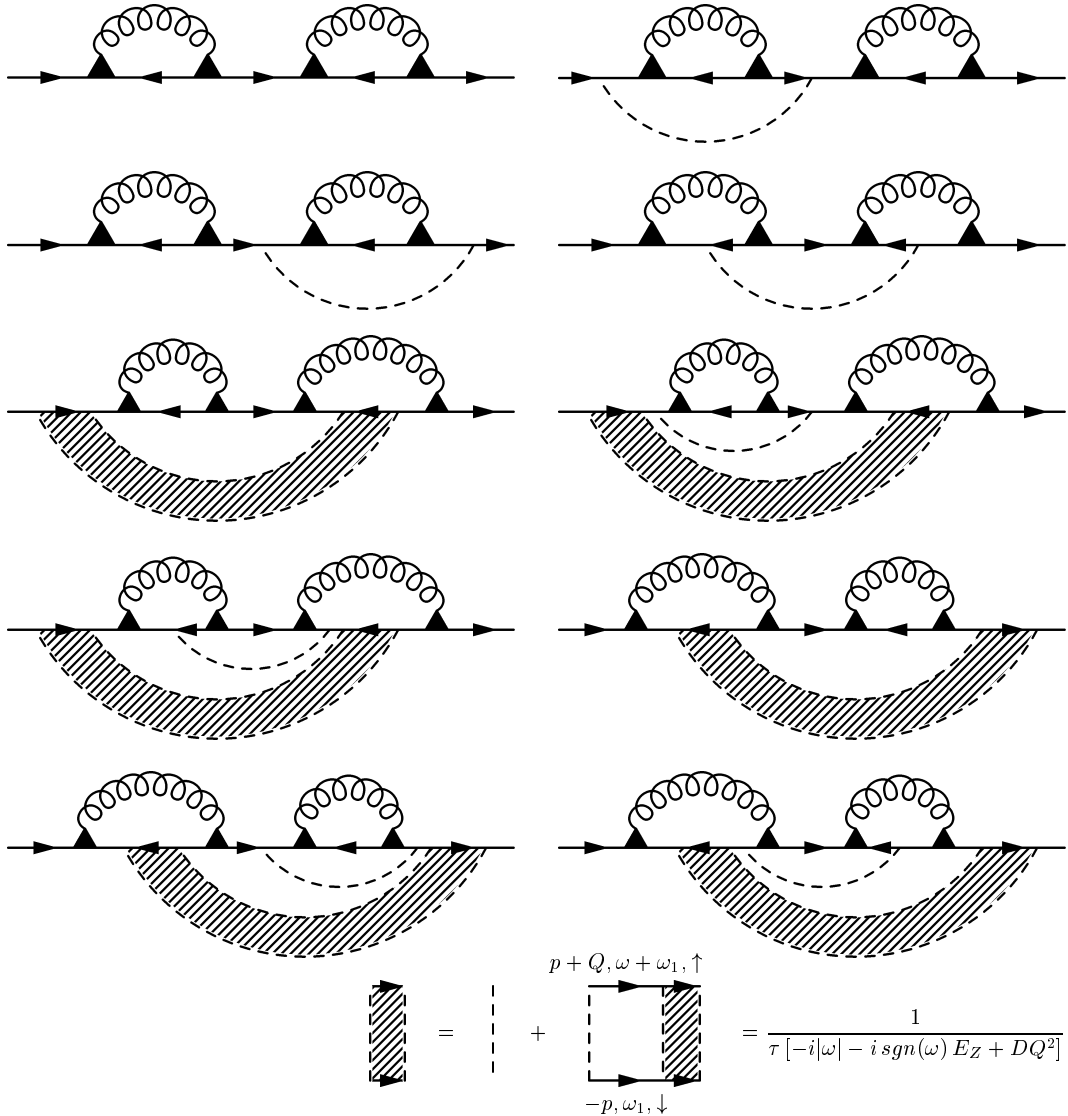


FIG. 7. Diagrams for the second order corrections to the DoS. Diagrams irreducible with respect to the curly lines, similar to Fig. 4a,b, are negligible for the reason discussed in the end of Sec. II.

As well as $1D$ case, the perturbation theory fails to describe the DoS in the vicinity of E^* in two dimensions. It is noteworthy that the singularity described by Eq. (3.13) is much more pronounced than that of the normal metal ($T > T_c$) which arises due to the superconducting fluctuations and it is of the order of $g^{-1} \ln[\ln(\omega \pm E_Z)]$, see Ref. 4.

The enhancement of this singularity results directly from the isolated pole in the propagator of the superconducting fluctuations, see Eqs. (3.2) and (3.8) rather than in the branch cuts of Ref. 4.

B. Non-perturbative results

1. Derivation of self-consistency equations

We start summation of the perturbation theory terms from the series of diagrams for DoS presented on Fig. 8. Such diagrams dominate in each order of the perturbation theory in comparison with those of the same order but including irreducible with respect to curly lines elements, similar to Fig. 4a,b. The later statement can be justified by arguments similar to the analysis of diagrams Fig. 8 presented in the end of Sec. II.

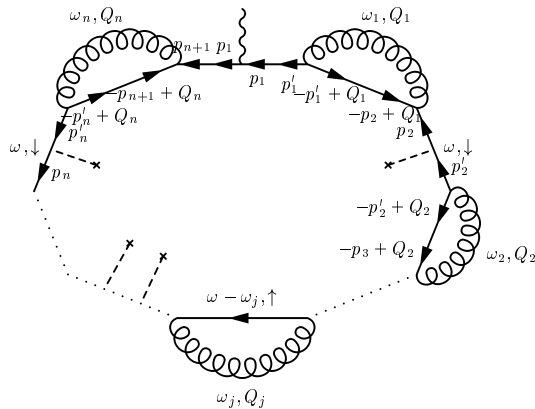


FIG. 8. Structure of the k -th order perturbation theory. Vertical wiggly line on the upper Green function corresponds to cutting this GF into two lines and fixing its frequency ω .

The diagram of the k -th order of the perturbation theory, Fig. 8, contains k curly lines that stand for the fluctuation propagator $\Lambda(\omega_j, Q_j)$ in Eq (3.2) ($1 \leq j \leq k$). It also contains $(2k + 1)$ GF. Before averaging over disorder, each GF $G_\sigma(\omega; p, p')$ depends on two momenta (initial p and final p') and on the direction of the spins $\sigma = \pm \equiv \uparrow, \downarrow$. Contribution of this diagram to the DoS of \downarrow electrons $\delta\nu_\downarrow(\omega)$ at positive energy $\omega > 0$ is

$$\begin{aligned} \delta\nu_\downarrow^{(k)}(\omega) &= -\frac{\text{sgn}(\omega)}{\pi} \text{Im} \int \frac{d\omega_1 d\omega_2 \cdots d\omega_k}{(2\pi)^k} \int (dp_1)(dp_1') \cdots (dp_{k+1}) \int (dQ_1)(dQ_2) \cdots (dQ_k) \\ &\times G_\downarrow(\omega; p_{k+1}, p_1) \prod_{j=1}^k \Lambda(\omega_j, Q_j) G_\downarrow(\omega; p_j, p_j') G_\uparrow(-\omega + \omega_j; -p_j' + Q_j, -p_{j+1} + Q_j). \end{aligned} \quad (3.14)$$

Disorder averaging of the product of the Green functions in Eq. (3.14) and of the superconducting propagator Λ can be carried out independently, since their correlation gives rise to non-singular corrections containing additional smallness $1/(\epsilon_F \tau)$.

For the sake of convenience we introduce $G^{R(A)}(\omega; p, p')$: retarded (advanced) GF at $E_Z = 0$. In the absence of spin-orbit scattering the Green functions $G^{R(A)}(\omega; p, p')$ from Eq. (3.14) can be presented through $G^{R(A)}$ as

$$G_\sigma(\omega; p, p') = \begin{cases} G^R(\omega + \sigma E_Z/2; p, p') & \omega > 0 \\ G^A(\omega + \sigma E_Z/2; p, p') & \omega < 0 \end{cases} \quad (3.15)$$

After substituting Eqs. (3.15) and (3.8) into Eq. (3.14), one can integrate over all intermediate frequencies ω_j , because the fluctuation propagator $\Lambda(\omega_j, Q_j)$ has simple poles at $\omega_j = \pm \Omega \mp iDQ_j^2$. According to Eq. (3.15), $G_\downarrow(\omega; p, p')$ in Eq. (3.14) is retarded ($\omega > 0$). In order to get the advanced GF from $G_\uparrow(\omega_j - \omega; -p_j' + Q_j, -p_{j+1} + Q_j)$ we choose the pole in $\Lambda(\omega_j; Q_j)$ with positive real part, $\omega_j = \Omega - iDQ_j^2$. (One can check that another pole leads to the product of the retarded functions, which vanish after the disorder averaging.) Using Eqs. (3.8) and (2.8) and introducing short-hand notation

$$\omega_{Q_j} \equiv -\omega + 2E^* - iDQ_j^2, \quad (3.16)$$

we can present $\delta\nu_{\downarrow}(\omega)$ at $\omega > 0$ as

$$\begin{aligned} \delta\nu_{\downarrow}^{(k)}(\omega) &= -\frac{1}{\pi} \left(\frac{\Delta^2}{\nu_0\Omega} \right)^k \text{Im} \int (dp_{k+1}) G^R(\omega; p_{k+1}, p_1) \prod_{j=1}^n (dp_j)(dp'_j)(dQ_j) \\ &\quad G^R(\omega; p_j, p'_j) G^A(\omega_{Q_j}; -p'_j + Q_1, -p_{j+1} + Q_j). \end{aligned} \quad (3.17)$$

Averaging Eq. (3.17) over disorder and using the identity

$$\int (dp_1) G^R(\omega; p_1, p'_1) G^R(\omega; p_{k+1}, p_1) = -\frac{\partial}{\partial\omega} G^R(\omega; p_{k+1}, p'_1), \quad (3.18)$$

we obtain

$$\begin{aligned} \langle \delta\nu_{\downarrow}^{(k)}(\omega) \rangle &= -\frac{1}{\pi} \left(\frac{\Delta^2}{\nu_0\Omega} \right)^k \left(\frac{1}{2k} \right) \frac{\partial}{\partial\omega} \text{Im} \left\langle \int \prod_{j=1}^k (dQ_j)(dp_j)(dp'_j) \right. \\ &\quad \left. \times G^R(\omega; p_j, p'_j) G^A(\omega_{Q_j}; -p'_j + Q_j, -p_{j+1} + Q_j) \right\rangle. \end{aligned} \quad (3.19)$$

The role of the factor $1/k$ in Eq. (3.19) is to cancel the multiple counting: there are k retarded GF in Eq. (3.19), and application of the operator ∂_{ω} to any one of them leads to Eq. (3.17). In addition, Eq. (3.19) includes terms like $\partial G^A/\partial\omega$. One can check that they give exactly the same contribution as terms which contain $\partial G^R/\partial\omega$. Additional factor $1/2$ takes these contributions into account.

Using a conventional trick $1/k = \int_0^1 \eta^k d\eta$, (see Ref. 7), one can present $\langle \delta\nu_{\downarrow}^{(k)}(\omega) \rangle$ in a form

$$\begin{aligned} \langle \delta\nu_{\downarrow}^{(k)}(\omega) \rangle &= -\frac{1}{2\pi\tau} \frac{\Delta^2}{\nu_0\Omega} \text{Im} \frac{\partial}{\partial\omega} \int_0^1 d\eta \int (dQ)(dp) \langle G^R(\omega; p) \rangle \langle G^A(\omega_Q; -p + Q) \rangle \\ &\quad \times \gamma_{\omega}^{(k)}(\tilde{\omega}_Q, Q), \end{aligned} \quad (3.20)$$

where short hand notation

$$\tilde{\omega}_Q = \omega - \omega_Q = 2\omega - 2E^* + iDQ^2 \quad (3.21)$$

is used and ω_Q is defined in Eq. (3.16). Similar equation holds for spin up and negative ω . In this case one should use $\tilde{\omega}_Q = -2\omega - 2E^* + iDQ^2$.

The vertex $\gamma^{(k)}$ can be written using Fig. 9. The rules of reading diagrams on Figs. 9 and 10 are slightly different from the conventional rules we used before: (i) to each curly line corresponds factor $\eta\Delta^2/(\nu_0\Omega)$; (ii) no summation over the frequencies is implied: each retarded GF bears frequency ω , each advanced GF bears frequency ω_Q given by Eq. (3.16); (iii) each interaction with curly lines changes retarded Green function to advanced and back. The resulting expression reads:

$$\begin{aligned} \gamma_{\omega}^{(k)}(\tilde{\omega}_Q, Q) &= \tau \left(\eta \frac{\Delta^2}{\nu_0\Omega} \right)^{k-1} \left\langle \int \prod_{j=1}^{k-1} (dQ_j)(dp_j)(dp'_j) \right. \\ &\quad G^R(\omega; p_j, p'_j) G^A(\omega_{Q_j}; -p'_j + Q_j, -p_{j+1} + Q_j) \\ &\quad \left. \times G^R(\omega; p'_1, p) G^A(\omega_Q; -p'_k + Q, -p + Q) \right\rangle. \end{aligned} \quad (3.22)$$

Note that the averaged product of GFs in the integrand of Eq. (3.22) does not depend on p . We can thus perform in Eq. (3.20) the integration over p . As a result, Eq. (3.22) takes a form

$$\frac{\delta\nu}{\nu_0} = -\frac{\Delta^2}{\nu_0\Omega} \text{Im} \frac{\partial}{\partial\omega} \int_0^1 d\eta \int (dQ) \gamma(\tilde{\omega}_Q, Q), \quad (3.23)$$

where

$$\gamma(\tilde{\omega}_Q, Q) = \sum_{k=1}^{\infty} \gamma^{(k)}(\tilde{\omega}_Q, Q). \quad (3.24)$$

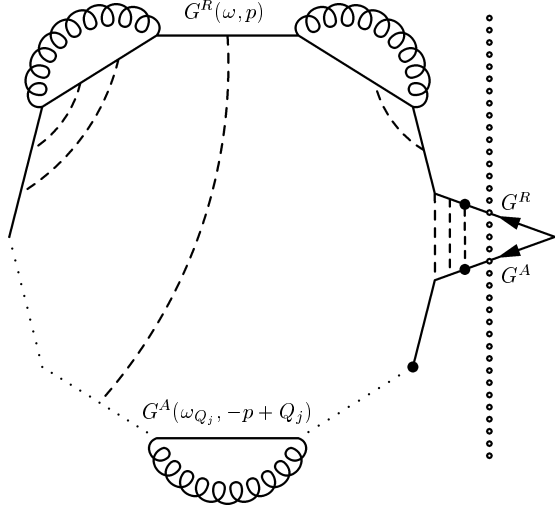


FIG. 9. Structure of the $\gamma^{(k)}$. Three points defining vertex are denoted by thick dots.

Our goal is to evaluate $\gamma(\tilde{\omega}_Q, Q)$ self-consistently. The difficulty is that diagrammatic series for γ contains other elements except γ itself, see Fig. 10.

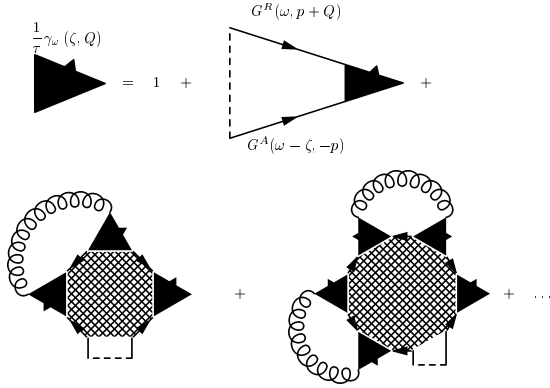


FIG. 10. Diagrammatic equation for the vertex $\gamma_\omega(\zeta, Q)$.

These elements are known as Hikami boxes¹⁴. The simplest Hikami box $B^{(2)}$, which appears already in second order of the perturbation theory for $\delta\nu$, is the integral (dp) of a sum of three diagrams shown on Fig. 11

$$B^{(2)}(\omega_1, \omega_2, Q_1, Q_2) = \frac{1}{(2\pi\nu_0)^3} [-i(\omega_1 + \omega_2) + D(Q_1^2 + Q_2^2)]. \quad (3.25)$$

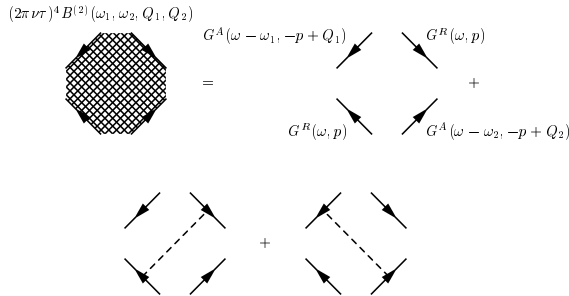


FIG. 11. Second order Hikami box $B^{(2)}$.

The third order Hikami box, $B^{(3)}$, is given by the momentum integral (dp) of a sum of sixteen diagrams of Fig. 12:

$$B^{(3)}(\omega_1, \omega_2, \omega_3; Q_1, Q_2, Q_3) = -\frac{2}{(2\pi\nu_0)^5} [-i(\omega_1 + \omega_2 + \omega_3) + D(Q_1^2 + Q_2^2 + Q_3^2)]. \quad (3.26)$$

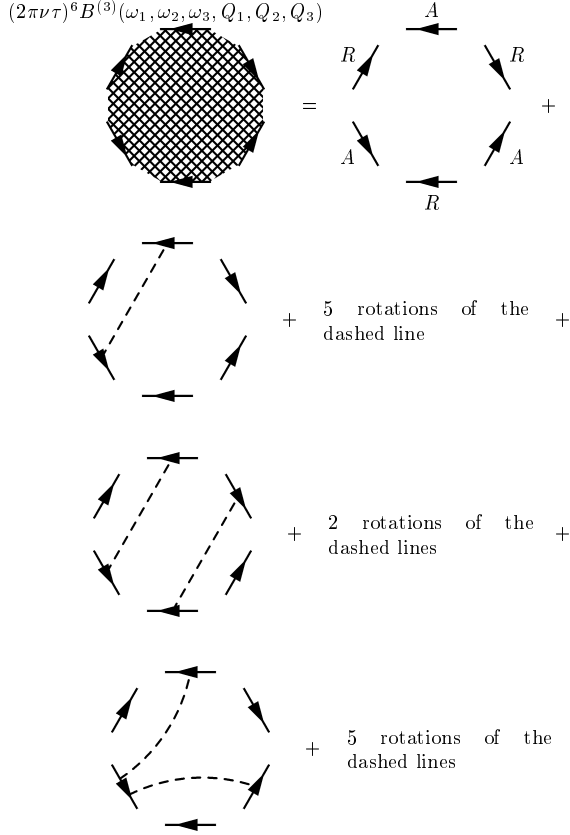


FIG. 12. Third order Hikami box $B^{(3)}$. Momenta and frequencies in the Green functions are arranged similar to Fig. 11.

The equation for the vertex $\gamma(\tilde{\omega}_Q, Q) \equiv \gamma_\omega(\zeta = \tilde{\omega}_Q, Q)$ that determines correction to the DoS [Eq. (3.23)]:

$$\begin{aligned} \frac{1}{\tau} \gamma_\omega(\zeta, Q) &= 1 + \left(\frac{1}{\tau} + i\zeta - DQ^2 \right) \gamma_\omega(\zeta, Q) \\ &+ \eta \left(\frac{\Delta^2}{\nu_0 \Omega} \right) \int (dQ_1) (2\pi\nu_0)^3 B^{(2)}(\tilde{\omega}_Q, \tilde{\omega}_{Q_1}, Q, Q_1) \gamma^2(1) \gamma_\omega(\zeta, Q) \\ &+ \eta^2 \left(\frac{\Delta^2}{\nu_0 \Omega} \right)^2 \int \int (dQ_1)(dQ_2) (2\pi\nu_0)^5 B^{(3)}(\tilde{\omega}_Q, \tilde{\omega}_{Q_1}, \tilde{\omega}_{Q_2}, Q, Q_1, Q_2) \\ &\times \gamma^2(1) \gamma^2(2) \gamma_\omega(\zeta, Q) + \dots, \end{aligned} \quad (3.27)$$

where $\gamma(j) = \gamma_\omega(\tilde{\omega}_{Q_j}, Q_j)$ with $\tilde{\omega}_{Q_j}$ determined by Eq. (3.21). We introduced extra variable ζ in order to separate the external energy ω and the integration variable in Eq. (3.27) and further.

Hikami box of the k -th order $B^{(k)}$ is given by a sum of diagrams (of the type of Figs. 11 and 12) which contain $2k$ vertices. Strictly speaking, $B^{(k)}$ depends on $2k - 1$ sets of momentum and energy transfer (ω, Q) . However, in order to evaluate the DoS correction given by diagrams Fig. 8, we can restrict ourselves by Hikami boxes that depend only

on k sets (ω_j, Q_j) , $1 \leq j \leq k$: (ω_j, Q_j) and $(-\omega_j, -Q_j)$ characterize neighboring vertices. Equations (3.25) and (3.26) allow us to conjecture that $B^{(k)}$ at arbitrary k has a form

$$B^{(k)}\{\omega_j, Q_j\} = \frac{C_k}{(2\pi\nu_0)^{2k-1}} \sum_{j=1}^k (-i\omega_j + DQ_j^2), \quad (3.28)$$

where C_k are numerical coefficients.

We are not going to determine coefficients C_k directly. An important feature of Hikami boxes is that they are local objects, determined by distances smaller or of the order of the mean free path l . Therefore, the coefficients C_k in Eq. (3.28) do not depend on the dimensionality. Therefore, we can compare the exact solution of 0-D problem, Sec. II, with the sum of perturbation theory series involving coefficients C_k and thus find those coefficients.

Equation (3.27) can be rewritten in terms of C_k as

$$\begin{aligned} (-i\zeta + DQ^2)\gamma_\omega(\zeta, Q) &= 1 + (-i\zeta + DQ^2)\gamma_\omega(\zeta, Q) \sum_{k=1}^{\infty} C_k \left[\eta \frac{\Delta^2}{\nu_0 \Omega} \int (dQ_1) \gamma(1)^2 \right]^k \\ &+ \gamma_\omega(\zeta, Q) \sum_{k=1}^{\infty} k C_k \left[\eta \frac{\Delta^2}{\nu_0 \Omega} \int (dQ_1) \gamma_\omega(\tilde{\omega}_{Q_1}, Q_1)^2 \right]^{k-1} \int (dQ_2) (-i\tilde{\omega}_{Q_2} + DQ_2^2) \gamma_\omega(\tilde{\omega}_{Q_2}, Q_2)^2. \end{aligned} \quad (3.29)$$

Introducing the function, $f(x)$

$$f(x) = - \sum_{k=1}^{\infty} C_k x^k + 1, \quad (3.30)$$

we obtain a simple equation for $\gamma_\omega(\zeta, Q)$

$$(-i\zeta + DQ^2)\gamma_\omega(\zeta, Q)f(\beta_0) + \gamma_\omega(\zeta, Q)\beta_1 f'(\beta_0) = 1, \quad (3.31)$$

where β_0 and β_1 are connected with γ by

$$\begin{aligned} \beta_0(\omega) &= \eta \frac{\Delta}{\nu_0 \Omega} \int (dQ) \gamma_\omega^2(\tilde{\omega}_Q, Q), \\ \beta_1(\omega) &= \eta \frac{\Delta}{\nu_0 \Omega} \int (dQ) \gamma_\omega^2(\tilde{\omega}_Q, Q) (-i\tilde{\omega}_Q + DQ^2). \end{aligned} \quad (3.32)$$

One can use Eq. (3.31) to present $\gamma_\omega(\zeta, Q)$ in the form

$$\gamma_\omega(\zeta, Q) = \frac{Z(\omega)}{-i\zeta + DQ^2 + 2m(\omega)}, \quad (3.33)$$

where parameters Z and m are determined as

$$Z(\omega) = \frac{1}{f(\beta_0(\omega))}, \quad 2m(\omega) = \beta_1(\omega) \frac{f'(\beta_0(\omega))}{f(\beta_0(\omega))}. \quad (3.34)$$

It was already mentioned that the Hikami boxes $B^{(n)}$ and thus coefficients C_n as well as the function $f(x)$ do not depend on the number of dimensions d . In contrast, ω -dependence of parameters β_0 , β_1 and m are different at different dimensions. Let us first consider 0D case in order to determine $f(x)$ explicitly. At $d = 0$ one has to abolish integration over Q in Eq. (3.32) and substitute inverse mean level spacing δ^{-1} for ν_0 and $2(\omega - E^*)$ for $\tilde{\omega}_Q$. The vertex γ can be determined straightforwardly

$$\gamma_\omega(\zeta) = \int \frac{d\epsilon_i}{2\pi} G_{i\downarrow}(\omega) G_{i\uparrow}^{0*}(\omega - E_Z - \zeta), \quad (3.35)$$

where 0D GF $G_{i\sigma}$ and $G_{i\sigma}^0$ are determined by Eq. (2.12) [Eq. (2.13) for W_0 should be multiplied by $\sqrt{\eta}$] and by Eq. (2.5) respectively. Substitution of Eqs. (2.12) and (2.5) into Eq. (3.35) gives after the integration over ϵ_i

$$\gamma_\omega(\zeta) = \frac{1}{2} \left[F_0 \left(\frac{\omega - E^*}{W_0} \right) + 1 \right] \frac{1}{-i\zeta + i(\omega - E^*) [1 - 1/F_0(\frac{\omega - E^*}{W_0})]}, \quad (3.36)$$

where the function $F_0(x)$ is given by Eq. (2.15), E^* is determined by Eq. (1.7), and $W_0^2 = \eta\bar{\delta}\Delta^2/\Omega$. By comparing Eq. (3.36) with Eq. (3.33) we immediately obtain $Z(\omega)$ and $m(\omega)$ for zero dimensions:

$$Z_0(\omega) = \frac{F_0\left(\frac{\omega-E^*}{W_0}\right) + 1}{2}, \quad (3.37)$$

$$m_0(\omega) = i(\omega - E^*) \frac{F_0\left(\frac{\omega-E^*}{W_0}\right) - 1}{2F_0\left(\frac{\omega-E^*}{W_0}\right)}. \quad (3.38)$$

On the other hand, from zero dimensional version of Eq. (3.32) at $\zeta = 2\omega - 2E^*$ we can determine β_0 and β_1 :

$$\beta_0 = \frac{1}{4F_0^2}, \quad \beta_1 = -2i\omega = \frac{-i\omega}{F_0^2}. \quad (3.39)$$

Now we are in state to determine the function $f(x)$ from Eq. (3.30). We express F_0 through β_0 , substitute it into Eq. (3.37) for Z_0 and use the connection Eq. (3.34) between $Z_0(\omega)$ and $f(\beta_0)$. As a result we have

$$f(x) = \frac{1}{2x} - \frac{1}{F_0(2x)} = \frac{1}{2x} - \frac{\sqrt{1-4x}}{2x}. \quad (3.40)$$

This functional dependence which remains the same at all dimensions, can be used to evaluate $\delta\nu_\downarrow(\omega)$ for $d = 1, 2$.

Equations (3.23), (3.32) – (3.34) and (3.40) constitute complete set allowing to find the DoS in any dimensions. One has to substitute Eq. (3.33) into Eq. (3.32), and find functions $Z(\omega)$ and $m(\omega)$ self-consistently with the help of Eqs. (3.34) and (3.40). The result should be substituted in Eq. (3.23) which gives the final non-perturbative answer for the DoS. In the following subsection, this program will be carried out for 1D (wires) and 2D (films) systems.

2. Solution of self-consistency equations

We substitute Eq. (3.33) into Eqs. (3.32) and (3.23) and perform integration over the wavevectors Q . Equation (3.23) acquires the form

$$\frac{\delta\nu_\sigma}{\nu_0} = -2 \frac{\partial}{\partial\omega} \text{Im} \int_0^1 d\eta \frac{M_d[-i\omega + m(\omega, \eta)]}{f[\beta_0(\omega, \eta)]}. \quad (3.41)$$

Here, we used Eq. (3.34) and introduced dimensionless frequency and mass

$$\omega \rightarrow \frac{\omega + \sigma E^*}{W_d}, \quad m \rightarrow \frac{m}{W_d}. \quad (3.42)$$

The relevant energy scales, which, as we will see below, are the widths of the tunneling anomaly, are given by

$$W_1 = 3 \left(\frac{\Delta^2}{16\nu_1\Omega\sqrt{D}} \right)^{2/3}, \quad W_2 = \frac{\Delta^2}{4g\Omega}, \quad (3.43)$$

where Ω is given by Eq. (2.8), D is the diffusion coefficient, $\nu_1 = (mp_F S)/(2\pi^2)$ is the one dimensional density of states per unit spin (S is the cross-section of the wire), and $g = 4\pi\nu_2 D$ is the dimensionless conductance¹⁵. The latter is related to the normal state resistance of the film as $g = 25.4k\Omega/R_\square$.

Dimensionless functions in Eq. (3.41), $M_d(x)$, are defined as

$$M_1(x) = \frac{2}{\sqrt{3x}}, \quad M_2(x) = \ln\left(\frac{4g}{x}\right). \quad (3.44)$$

To find M_2 we cut off the logarithmic divergence at large momenta Q by the condition $DQ^2 \lesssim \Delta$, which determines the applicability of a single pole approximation (3.8), and neglected the factor $\Delta/\Omega \simeq 1$ in the argument of the logarithm.

Using the same notation, we obtain from Eqs. (3.32) and (3.34)

$$\beta_0(\omega, \eta) \{f[\beta_0(\omega, \eta)]\}^2 = -\eta M'_d[-i\omega + m(\omega, \eta)] \quad (3.45a)$$

$$m \{f[\beta_0(\omega, \eta)]\}^3 = \eta f'[\beta_0(\omega, \eta)] \{M_d[-i\omega + m(\omega, \eta)] + m(\omega, \eta) M'_d[-i\omega + m(\omega, \eta)]\}. \quad (3.45b)$$

Equation (3.40) allows to formally solve Eq. (3.45a):

$$\beta_0 = -\frac{\eta M'_d(-i\omega + m)}{[1 - \eta M'_d(-i\omega + m)]^2}, \quad (3.46a)$$

$$f(\beta_0) = 1 - \eta M'_d(-i\omega + m), \quad (3.46b)$$

$$\frac{f'(\beta_0)}{[f(\beta_0)]^3} = \frac{1}{1 + \eta M'_d(-i\omega + m)}. \quad (3.46c)$$

We can now substitute Eq. (3.46c) into Eq. (3.45b) and obtain after simple algebra

$$m(\omega, \eta) = \eta M_d[-i\omega + m(\omega, \eta)]. \quad (3.47)$$

Further calculation are substantially simplified due to the fact that the integrand in Eq. (3.41) can be presented as a total derivative with respect to η . In order to demonstrate this, we differentiate both sides of Eq. (3.47) with respect to η :

$$\frac{\partial m}{\partial \eta} = M_d(-i\omega + m) + \eta M'_d(-i\omega + m) \frac{\partial m}{\partial \eta}. \quad (3.48)$$

Finding $\partial m/\partial \eta$ from Eq. (3.48), we notice with the help of Eq. (3.46b) that it coincides with the integrand in Eq. (3.41). Integration in Eq. (3.41) can be immediately performed and we obtain

$$\frac{\delta \nu_\sigma}{\nu_0} = -2 \frac{\partial}{\partial \omega} \text{Im } m(\omega, \eta = 1). \quad (3.49)$$

Finally we put $\eta = 1$ in Eq. (3.47), differentiate both sides of this equation with respect to ω , and substitute the result for $\partial m/\partial \omega$ into Eq. (3.49). After restoration of original units for ω according to Eq. (3.42), we obtain for the density of states $\nu_\sigma(\omega) = \nu_0 + \delta \nu_\sigma(\omega)$ the following result

$$\frac{\nu_\sigma(\omega)}{\nu_0} = F_d \left(\frac{\omega + \sigma E^*}{W_d} \right) \quad (3.50)$$

where $\sigma = \pm 1$ corresponds to the spin-up and spin-down densities of states respectively, and the widths of the singularity W_d are defined in Eq. (3.43). Dimensionless function $F_d(x)$ is given by

$$F_d(x) = \text{Re} \frac{1 + z(x)}{1 - z(x)} \quad (3.51a)$$

where function $z(x)$ is implicitly defined as the solution of equations

$$\begin{aligned} z(x) &= M'_d[-ix + y(x)], \\ y(x) &= M_d[-ix + y(x)], \end{aligned} \quad (3.51b)$$

with functions $M_d(x)$ being defined in Eq. (3.44). If Eq. (3.51b) has several solutions, one has to choose the one reproducing the perturbation theory at $x \gg 1$ and remaining on the same list of the Riemann surface at small x .

In 1D case, Eq. (3.51b) can be rewritten as a cubic equation and solved using the Cardano formula which yields universal (independent on ν_1 and D) expression for the shape of the singularity:

$$\begin{aligned} F_1(x) &= 1 - \frac{2}{3} \text{Re} \left[1 - ix \left(\sqrt[3]{1 + y(x)} + \sqrt[3]{1 - y(x)} \right) \right]^{-1} \\ y(x) &= \sqrt{1 + ix^3}. \end{aligned} \quad (3.52)$$

Functions $\sqrt[3]{z}$ in Eq. (3.52) are defined to map complex plane $-\pi < \arg(z) < \pi$ to $-\frac{\pi}{3} < \arg(z) < \frac{\pi}{3}$.

For the two-dimensional case, we obtain from Eqs. (3.51) and (3.44):

$$F_2(x) = \text{Re} \frac{1 - z(x)}{1 + z(x)}, \quad (3.53)$$

where $z(x)$ is the solution of the transcendental equation

$$z(x) = \frac{1}{-ix + \ln[4gz(x)]}. \quad (3.54)$$

Shape of the singularity in this case depends on the conductance g and, thus, is not universal. However, this dependence is rather weak. For $|\omega \pm E^*| \gg W_d$, Eqs. (3.52) and (3.53) match the perturbative results, Eqs. (3.11) and (3.13). Found energy dependence of the density of states is shown in Fig. 13.

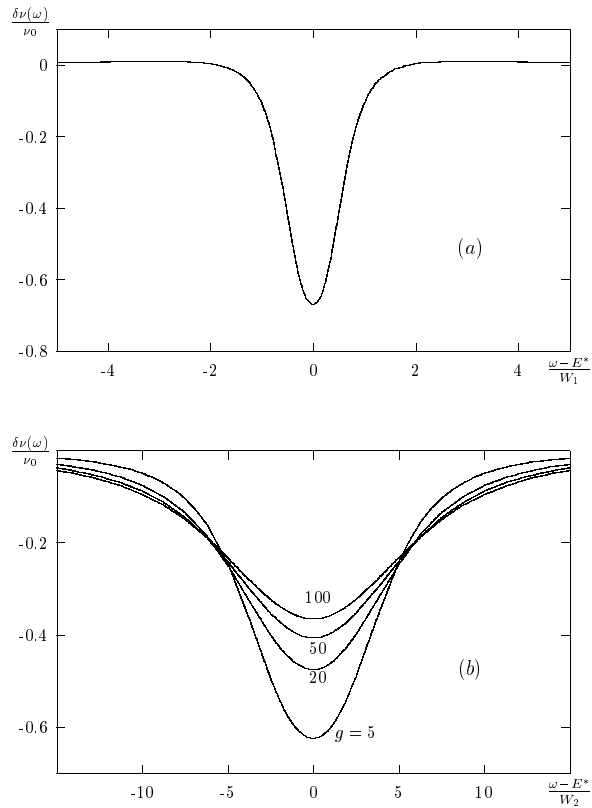


FIG. 13. Singularity in DoS for spin-down polarized electrons for (a) 1D, and (b) 2D systems. Widths of the singularity $W_{1,2}$ are given by Eq. (3.43), and the shape is defined by Eqs. (3.50), (3.52) and (3.53).

IV. QUALITATIVE DISCUSSION

In this section we will present a simple qualitative interpretation of the main results obtained in the previous sections. We believe that this simplified way of thinking provides instructive physical intuition even though it fails to give completely quantitative description.

It has been already emphasized in the beginning of section Sec. II that the ground state of the system above the paramagnetic limit has the structure similar to that of a non-interacting system. All the mixing of the noninteracting states caused by the interaction part of the Hamiltonian (2.1) is perturbative. We can neglect it completely in a rough approximation and consider the electrons occupying orbitals with orbital energies $\epsilon_i < -E_Z/2$, see Fig. 2, to be “frozen”. As soon as the spin down electron tunnels onto an orbital $0 < \epsilon_0 < E_Z/2$, see Fig. 2, the electron pair on this orbital is created. Due to the interaction, this pair can mix with all the empty states, $\epsilon_i > E_Z/2$. It is this mixing which gives rise to the singularity in the DoS. On the other hand, within the same approximation, all the electrons on the orbitals $\epsilon_i < -E_Z/2$ can still be considered as “frozen”. (This approximation is similar in spirit to the well-known Cooper procedure¹⁶.)

Thus, we arrive to the following recipe for the evaluation of the energy of one electron excitation. First we have to find the eigenenergies $E_{(2)}^j(\epsilon_0)$ of the two-electron problem within the Hilbert space consisting of orbital ϵ_0 and of all

the orbitals $\epsilon_i > E_Z/2$, see Fig. 14. (This energy spectrum naturally depends on ϵ_0 as parameter.) Then, the energies $E_{\downarrow}^j(\epsilon_0)$ of the one particle excitation, corresponding to the introduction of electron onto the orbital ϵ_0 are

$$E_{\downarrow}^j(\epsilon_0) = E_{(2)}^j(\epsilon_0) - \left(\epsilon_0 - \frac{E_Z}{2} \right), \quad (4.1)$$

since the total energy of the electron which occupied this orbital before the tunneling event was $\epsilon_0 - E_Z/2$, while the state of the rest of the electrons did not change. Accordingly, the density of states for spin-down electrons is given by

$$\nu_{\downarrow}(\omega) \simeq \sum_{j, \epsilon_0} \delta \left[\omega - E_{\downarrow}^j(\epsilon_0) \right]. \quad (4.2)$$

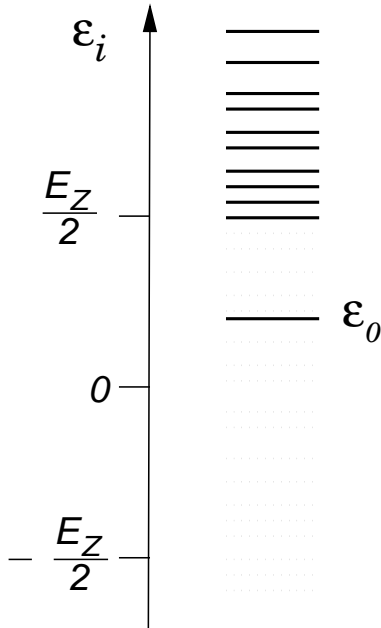


FIG. 14. Hilbert space for the solution of two - electron problem. All the orbitals (dotted lines) with $\epsilon_i < -E_Z/2$ are excluded since they are occupied by “frozen” electron pairs and the orbitals $-E_Z/2 < \epsilon_i < E_Z/2, \epsilon_i \neq \epsilon_0$ are excluded because single occupied orbitals are not affected by the interaction (2.1).

Now, we have to find the spectrum of two electron eigenenergies $E_{(2)}^j(\epsilon_0)$. Since the interaction in the Hamiltonian involves only the spin-singlet orbitals, the wave function of the electron pair ψ can be labeled by one orbital index and it is governed by the Schrödinger equation:

$$E_{(2)}^j \psi_i = 2\epsilon_i \psi_i - \lambda \bar{\delta} \sum_j \psi_j. \quad (4.3)$$

The eigenenergies $E_{(2)}^j$ can be determined from the following equation

$$\frac{\bar{\delta}}{2\epsilon_0 - E_{(2)}^j} + \sum_{\epsilon_i > E_Z/2} \frac{\bar{\delta}}{2\epsilon_i - E_{(2)}^j} = \frac{1}{\lambda}. \quad (4.4)$$

For low-lying eigenstates $E_{(2)}^j < E_Z$, one can substitute the summation in Eq. (4.4) by the integration. Given the high-energy cut-off ω_c , it yields

$$\frac{2\bar{\delta}}{2\epsilon_0 - E_{(2)}^j} = \ln \left(1 + \frac{E_Z - E_{(2)}^j - \Delta_b}{\Delta_b} \right), \quad (4.5)$$

where $\Delta_b = \omega_c \exp(-2/\lambda)$ is the binding energy of the Cooper pair.

As we will see in a moment, $|2\epsilon_0 - E_{(2)}^j| \gg \bar{\delta}$, and, therefore, the logarithm in Eq. (4.5) should be also small and it can be expanded in the Taylor series, $\ln(1+x) \approx x$, $|x| \ll 1$. Equation (4.5) is immediately simplified to

$$\frac{2\bar{\delta}}{2\epsilon_0 - E_{(2)}^j} = \frac{E_Z - \Delta_b - E_{(2)}^j}{\Delta_b},$$

and we obtain the solution for two relevant eigenenergies:

$$E_{(2)}^\pm(\epsilon_0) = \epsilon_0 + \frac{\Omega_b}{2} \pm \sqrt{\left(\frac{\Omega_b}{2} - \epsilon_0\right)^2 + 2\bar{\delta}\Delta_b}. \quad (4.6)$$

All the other two-electron states have energies larger than E_Z and they are not important for us. In Eq. (4.6) energy

$$\Omega_b = E_Z - \Delta_b \quad (4.7)$$

has the meaning of the energy of the bound state of the Cooper pair measured from the Fermi level. It plays the role of energy Ω from Eq. (2.8) in the rigorous solution. We will return to the discussion of the discrepancy between Eq. (4.7) and Eq. (2.8) later.

Substituting Eq. (4.6) into Eq. (4.1), we obtain the energy of one particle excitations

$$E_\downarrow^\pm(\epsilon_0) = E_b^* \pm \sqrt{\left(\frac{\Omega_b}{2} - \epsilon_0\right)^2 + 2\bar{\delta}\Delta_b}, \quad (4.8)$$

where the position of the singularity

$$E_b^* = \frac{E_Z + \Omega_b}{2} \quad (4.9)$$

is similar to the energy E^* in exact Eq. (2.11) up to the substitution $\Omega \rightarrow \Omega_b$.

According to Eqs. (4.2) and Eq. (4.8), the density of states *vanishes* in the energy strip $|E - E_b^*| < (2\bar{\delta}\Delta_b)^{1/2}$ – hard gap in the DoS is formed, compare with the exact result, Eq. (2.15). The origin of this tunneling anomaly is the avoided crossing of the two-electron state formed by the tunneling electron (energy $2\epsilon_0$) with the bound state of the Cooper pair (energy Ω_b).

It is also noteworthy that if a spin-up electron tunnels into the grain, it never finds the pair for itself, and, therefore, no tunneling anomaly happens in this case. It means that the overall DoS does not vanish but rather shows the suppression by a factor of two. However, for the spin-polarized electrons tunneling into the grain, we predict the complete suppression of the tunneling DoS.

The same arguments allow to justify the similar singularity, when spin-up electron with energy $-E_Z/2 < E < 0$ tunnels out from the system, while the spin down electrons tunneling from the system are not affected.

The qualitative consideration above grasps the correct physics, however it fails to describe the effect quantitatively, it predicts correctly neither the position nor the width of the gap. This is similar to the discrepancy between the binding energy Δ_b in the original Cooper procedure and the correct BCS gap Δ : all the electrons below the Fermi energy were frozen. To remedy this drawback, one has to employ a parametrically exact procedure described in Secs. II and III.

Let us now discuss the results obtained for the disordered bulk systems, Sec. III. They can be briefly summarized as follows: (i) Singularity in the DoS persists; (ii) its position does not change; (iii) energy scale of the singularity depends on both disorder and dimensionality, see Eq. (3.43).

In order to understand the physics behind the singularities in the bulk systems, let us recall the meaning of zero-dimensional approximation. Strictly speaking, it implies that during the time $t_E \simeq \hbar/E$, (where E is the energy scale relevant for the problem), diffusively moving electron can visit all the system. The characteristic time of this diffusion is $\simeq L^2/D$, (L is the characteristic size of the system) which means that zero-dimensional approximation is applicable provided that the energy scale E does not exceed the Thouless energy $E_c = \hbar D/L^2$. In our problem the relevant energy scale is the gap width W_0 from Eq. (2.13), and condition

$$1 > \frac{W_0}{E_c} \propto L^{2-d/2} \quad (4.10)$$

is definitely violated for the infinite systems $L \rightarrow \infty$, (here $d = 1, 2$ is the dimensionality of the system).

It is clear, that as soon as the condition (4.10) breaks down the geometrical size of the system L as well as its mean level spacing $\bar{\delta} = 1/(\nu_0 L^d)$ is not relevant since the electron can not diffuse during finite time $t_E = \hbar/E$ over the distance larger than $L_E = \sqrt{Dt_E}$. On the other hand, it effectively visits all the space on the scale smaller than L_E . Therefore, the following approximation holds: in order to understand the properties of the diffusive system associated with the energy scale E , we can separate the system into smaller patches of the size $L_E = \sqrt{\hbar D/E}$, and, then, apply zero-dimensional description to each patch independently, (assuming that different patches do not “talk” to each other).

Let us now apply this strategy to the problem in hand. First, we notice that the position of the singularity in 0D grain (2.11) does not depend on the size of the grain and therefore the singularity in each patch should be at the same energy E^* as in zero-dimensional systems. Second, level spacing $\bar{\delta}$ entering into the width of the singularity Eq. (2.13) does depend on the size of the patch

$$\bar{\delta} = \frac{1}{\nu_0 L_E^d}. \quad (4.11)$$

In this formula, scale L_E is itself determined by the width of the singularity, $E \simeq W_d$, so that the scale W_d has to be determined self-consistently. Substituting Eq. (4.11) into Eq. (2.13), we find

$$W_d \simeq \left(\frac{\Delta^2}{\nu_0 L_W^d \Omega} \right)^{1/2}; \quad L_W \simeq \left(\frac{D}{W_d} \right)^{1/2}. \quad (4.12)$$

Solving Eq. (4.12), we obtain

$$W_d \simeq \Delta \left(\frac{\Delta^{d/2}}{\nu_0 \Omega D^{d/2}} \right)^{\frac{2}{4-d}}, \quad (4.13)$$

which agrees with the rigorous results (3.43) for one- ($d = 1$) and two- ($d = 2$) dimensional systems. However, the quantitative description requires machinery like one used in Sec. III.

V. RELEVANT PERTURBATIONS

A. Spin-orbit scattering

In our previous consideration we assumed that electronic spin is a good quantum number, i.e., impurity scattering of electrons does not cause spin-flips. There are two sources of spin relaxation of conduction electrons: localized spins (paramagnetic impurities) and spin-orbit (SO) scattering of electrons by non-magnetic disorder. The latter is characterized by the scattering amplitude

$$iv_{so}([\mathbf{p}_f \times \mathbf{p}_i] \cdot \boldsymbol{\sigma})/p_F^2, \quad (5.1)$$

where \mathbf{p}_f and \mathbf{p}_i are final and initial momenta of an electron, and $\boldsymbol{\sigma}$ is the spin operator $\boldsymbol{\sigma} = (\hat{\sigma}_x, \hat{\sigma}_y, \hat{\sigma}_z)$ whose components are Pauli matrices. It acts on the spinor wave function of the electron.

Let us discuss the effect of SO scattering first starting with the qualitative physical picture. In the absence of both SO interactions and magnetic field two spin states which belong to a given orbital have the same energy. Magnetic fields splits this degeneracy. It was important for us that the splitting E_Z is exactly the same for all of the orbital states. Now let us turn on SO interaction. Without external magnetic field the states are still double degenerate due to the T-invariance (Kramers doublets¹⁷). Magnetic field is well known to split the Kramers doublets similar to how it splits pure spin states in the absence of SO interactions. The main difference is that this splitting is not exactly uniform any more (see e.g. Ref. 18). It is this dispersion of splittings that smears the DoS singularity. Zeeman splitting dominates the magnetic field effect on superconductivity only provided SO interaction is weak. However the DoS singularity turns out to be sensitive even to a weak SO scattering, since the characteristic SO energy (dispersion is splitting of Kramers doublets) should be compared with the width of the singularity W_d rather than with the splitting E_Z itself. The DoS for finite SO scattering can be evaluated in a way similar to our calculation in Sec. III B.

Cooperon (or vertex) is formed by two electron Green functions. In the absence of external magnetic field it is convenient to classify Cooper poles by the total spin of two electrons $\mathbf{S}_+ = (\boldsymbol{\sigma}_1 + \boldsymbol{\sigma}_2)/2$. Spin-orbit scattering does not affect the spin singlet part of the Cooperon ($\mathbf{S}_+^2 = 0$) because the spin-orbit scattering preserves T -invariance. However, this scattering leads to total spin relaxation, i.e., triplet ($\mathbf{S}_+^2 = 2$) component of Cooperon decays (pole in ω -plane is shifted from the real axis even for $Q = 0$)²⁰.

External magnetic field is coupled with the difference $\mathbf{S}_- = (\boldsymbol{\sigma}_1 - \boldsymbol{\sigma}_2)/2$ of two electron spins, and as a result we classified Cooperon by the eigenvalue of the operator $\mathbf{S}_- \cdot \mathbf{E}_Z$. These eigenvalues for $\mathbf{S}_-^2 = 2$ are E_Z , 0 , $-E_Z$ corresponding to $S_-^z = 1$, 0 , -1 and 0 for $\mathbf{S}_-^2 = 0$. Neither of those two classifications is exact when both magnetic field and SO scattering take place simultaneously: operators \mathbf{S}_+^2 and S_-^z do not commute. On the other hand, as it was already mentioned, we should assume that SO effect is weak. This allows us to evaluate Cooperon perturbatively.

Summing usual ladder diagrams and taking additional scattering amplitude Eq. (5.1) into account, we end up with an equation for 4×4 matrix of the Cooperon which we already discussed qualitatively:

$$\left[(-i\omega + DQ^2) \hat{I} + i\mathbf{E}_Z \cdot \mathbf{S}_- + \frac{2\mathbf{S}_+^2}{3\tau_{so}} \right] \hat{C} = \frac{\hat{I}}{\tau}, \quad (5.2)$$

where $\tau_{so} = 1/(2\pi\nu_0 v_{so}^2)$ is the time of the spin relaxation by SO scattering, matrix \hat{I} is the direct product $\hat{I} = \sigma_0^s \otimes \sigma_0^e$, where unit matrix σ_0^s is acting in the spin 2×2 space, and σ_0^e is a unit matrix in 2×2 space of the electron lines. Operators \mathbf{S}_\pm are defined as $2\mathbf{S}_+ = (\boldsymbol{\sigma}^s + \mathbf{n}\sigma_0^s) \otimes \sigma_0^e$ and $2\mathbf{S}_- = (\boldsymbol{\sigma}^s - \mathbf{n}\sigma_0^s) \otimes \sigma_z^e$, where $\mathbf{n} = (1_x, 1_y, 1_z)$ is the unit vector, and $\boldsymbol{\sigma}^s = (\sigma_x^s, \sigma_y^s, \sigma_z^s)$ are the Pauli matrices in the spin space.

Instead of diagonalizing Eq. (5.2), we can just evaluate correction to $C_{\uparrow(\downarrow)}^{-1}$,

$$C_{\uparrow}^{-1} \equiv [C^{-1}]_{\uparrow, \downarrow}^{\uparrow, \downarrow} \quad C_{\downarrow}^{-1} \equiv [C^{-1}]_{\downarrow, \uparrow}^{\downarrow, \uparrow} \quad (5.3)$$

in the first order of the perturbation theory in $(E_Z \tau_{so})^{-1} \ll 1$. This correction turns out to be $2/(3\tau_{so})$. As a result, SO scattering simply shifts the Cooper poles $C_{\uparrow(\downarrow)}$:

$$C_{\uparrow(\downarrow)}(\omega, Q) = \frac{1}{-i\omega \mp iE_Z + DQ^2 + \frac{2}{3\tau_{so}}}. \quad (5.4)$$

From Eq. (5.4) one can guess that the all the interesting results can be obtained from the results of Secs. II and III by substituting

$$\omega \rightarrow \omega + i\Gamma, \quad (5.5)$$

where Γ is the spin orbit rate

$$\Gamma = \frac{2}{3\tau_{so}}, \quad (5.6)$$

so that the final result for the density of states is

$$\frac{\nu_{\uparrow(\downarrow)}(\omega)}{\nu_0} = \text{Re} F_d \left(\frac{\omega \pm E^* + i\Gamma}{W_d} \right) \quad (5.7)$$

with W_d and E^* determined by Eqs. (2.13), (3.43), and (1.7), and dimensionless function F_d are given by Eqs. (2.15), (3.52) and (3.53). We notice that the DoS singularity gets smeared by SO scattering when $\Gamma \gtrsim W_d$. This is in contrast with conventional superconductivity which is known to be stable with respect to SO scattering since the latter does not violate T-invariance.

This guess turns to be correct. In order to demonstrate it one has to show that not only the Cooperon but also Hikami boxes from Sec. IIIB are modified according the rule (5.5). Taking into account the spin orbit scattering Eq. (5.1) in impurity lines on diagrams Figs. 11 and 12, we obtain

$$B^{(2)}(\omega_1, \omega_2, Q_1, Q_2) = \frac{1}{(2\pi\nu_0)^3} \left[-i(\omega_1 + \omega_2) + D(Q_1^2 + Q_2^2) + \frac{4}{3\tau_{so}} \right],$$

$$B^{(3)}(\omega_1, \omega_2, \omega_3; Q_1, Q_2, Q_3) = -\frac{2}{(2\pi\nu_0)^5} \left[-i(\omega_1 + \omega_2 + \omega_3) + D(Q_1^2 + Q_2^2 + Q_3^2) + 2\tau_{so} \right].$$

With the same rigor as in Sec. III B, we conjecture that

$$B^{(n)}\{\omega_j, Q_j\} = \frac{C_n}{(2\pi\nu_0)^{2n-1}} \sum_{j=1}^n \left(-i\omega_j + DQ_j^2 + \frac{2}{3\tau_{so}} \right),$$

therefore, rule (5.5) is satisfied which gives Eq. (5.7).

Finally we emphasize that, in Eq. (5.7) complex argument of the function $F_d(z)$ should be located on the physical sheet: $z = |z| \exp i\varphi$ and $-\pi < \varphi < \pi$. Thus, the functions $\sqrt[n]{z}$ in Eqs. (2.15) and (3.52) are defined to map complex plane $-\pi < \arg(z) < \pi$ to $-\frac{\pi}{d} < \arg(z) < \frac{\pi}{d}$.

B. Paramagnetic impurities, orbital effects of the magnetic field

The derivation in the previous section suggests that any physical mechanisms of violation of either T-invariance or conservation of spin will have similar effect on the DoS singularity. Indeed, in 0D and 1D cases in the presence of magnetic field H and paramagnetic spins, Eq. (3.10) takes the following form⁴

$$C(\omega, Q) = \frac{1}{-i\omega + DQ^2 + \frac{1}{\tau_{tot}}}, \quad (5.8)$$

where τ_{tot} is a combination of phase and spin relaxation effects

$$\frac{1}{\tau_{tot}} = \frac{1}{t_\varphi} + \frac{1}{t_s}. \quad (5.9)$$

Both SO scattering and spin exchange with paramagnetic impurities (τ_s) lead to spin relaxation:

$$\frac{1}{t_s} = \frac{2}{3} \left(\frac{1}{\tau_{so}} + \frac{1}{\tau_s} \right). \quad (5.10)$$

Phase may relax either due to inelastic processes or due to magnetic field effect on orbital motion of electrons:

$$\frac{1}{t_\varphi} = \frac{1}{\tau_\varphi} + \frac{1}{\tau_H}. \quad (5.11)$$

When the transverse dimension of the wire (size of the grain) a , exceeds mean free path l , τ_H can be estimated as^{4,22}

$$\frac{1}{\tau_H} = A \frac{\Omega_H^2}{E_T} \propto D \left(\frac{aH}{\phi_0} \right)^2. \quad (5.12)$$

Here $\phi_0 = \frac{hc}{2e} \simeq 2 \times 10^{-7} \text{Gs} \cdot \text{cm}^2$ is the superconductivity magnetic flux, E_T is the "transverse" Thouless energy, $E_T = D/a^2$, and Ω_H is the Cooperon "cyclotron frequency" (cyclotron frequency for a particle which mass and charge equal to $(2D)^{-1}$ and $2e$ respectively)⁴.

$$\Omega_H = \frac{4DeH}{\hbar c} \quad (5.13)$$

Numerical coefficient A is not universal: it depends on the geometry of the superconductor, on the direction of magnetic field, etc.

Equation (5.8)–(5.13) are valid also for 2D films provided H is parallel to the film plane. In this case

$$\frac{1}{\tau_H} = \frac{a^2 \Omega_H^2}{48D} = \frac{D(eHa)^2}{3c^2 \hbar^2}. \quad (5.14)$$

Now, we again conjecture that Eq. (3.28) for Hikami boxes is still valid with addition of $1/\tau_{tot}$ to all DQ_j^2 . If so, Eq. (5.7) for DoS is still valid, but instead of Eq. (5.6) we should substitute

$$\Gamma = \frac{1}{\tau_{tot}} \quad (5.15)$$

Rate τ_φ^{-1} in Eq. (5.11) is the contribution of inelastic collisions. This contribution will be estimated in the next section. Evolution of the density of states with the rate $\alpha = \Gamma/W_d$ for different dimensions is shown in Fig. 15.

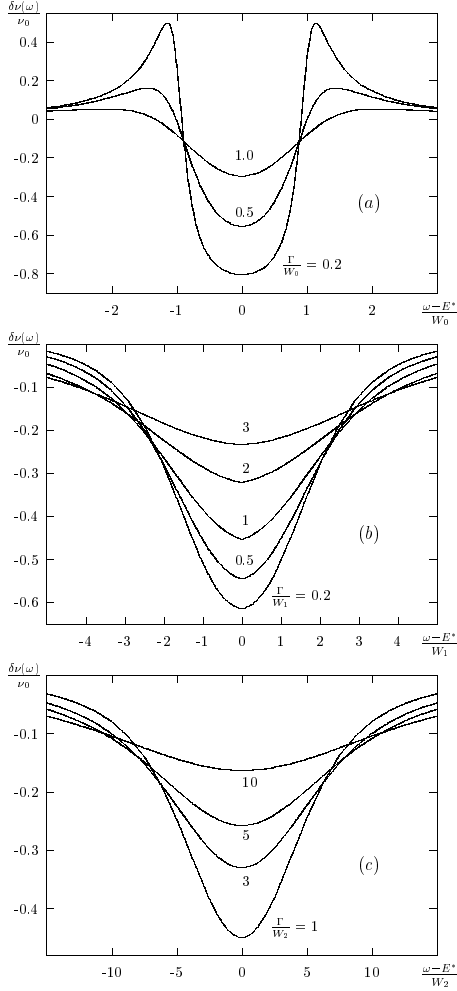


FIG. 15. Singularity in DoS for spin-down polarized electrons for (a) $0D$, and (b) $1D$ and (c) $2D$ systems for different values of dimensionless rate $\alpha = \Gamma/W_d$. The DoS in two dimensional case is plotted for conductance $g = 10$.

C. Finite temperature and inelastic processes

Our previous consideration, strictly speaking, applies only when temperature T equals to zero. Let us now discuss effects of finite T .

Temperature manifests itself through distribution of electrons in energy. This distribution substantially depends on T only for energies of the order of T . On the other hand, for tunneling anomalies at finite bias $eV \sim E^*$, Eq. (1.7), only low temperature region $T \ll E^*$ (recall that the Zeeman splitting E_Z as well as superconducting gap Δ are normally of the order of E^*) is of interest. Indeed, thermal broadening of the Fermi steps in the leads washes out any singularity as soon as T exceeds the width W of this singularity. Since the widths W_d , Eqs. (2.13) and (3.43), are much smaller than E^* , there will be already no anomaly of the tunneling current at $T \sim E^*$. On the other hand, at $T \ll E^*$ the equilibrium occupation number of a state with the energy of the order of E^* is exponentially small and thus can be neglected. Therefore, formally determined DoS, Eq. (3.50) is temperature independent up to terms of the order of $\exp(-E^*/T)$. However, the observable, namely tunneling conductance $\sigma_T(eV)$, depends on T through the Fermi distribution $n_F(\omega/T)$ in the leads. To evaluate the singular part $\delta\sigma_T(eV)$ of the tunneling conductance, one has to convolute $\delta\nu(\omega)$ with the derivative of the biased Fermi distribution:

$$\frac{\delta\sigma_T(eV)}{\sigma_T^0} = - \int d\omega \frac{\partial n_F(\frac{\omega-eV}{T})}{\partial\omega} \frac{\delta\nu_\uparrow(\omega) + \delta\nu_\downarrow(\omega)}{\nu_0} \quad (5.16)$$

Substitution of Eq. (3.50) into Eq. (5.16) yields for $\sigma_T = \sigma_T^0 + \delta\sigma_T$:

$$\frac{\sigma_T(eV)}{\sigma_T^0} = \int \frac{d\omega}{4T \cosh^2(\frac{\omega-eV}{2T})} \sum_{\sigma=\pm 1} \text{Re}F_d \left(\frac{\omega + \sigma E^* + i\Gamma}{W_d} \right) \quad (5.17)$$

To complete this discussion, let us estimate contribution of inelastic collisions of electrons, $1/\tau_\varphi$ Eq. (5.11), to Γ . Since we are dealing with rather highly excited states ($\omega \sim E^* \gg T$), relaxation rate $1/\tau_\varphi$ is determined by large energy transfer ($\sim E^*$), and thus is temperature independent. In all interesting cases $1/\tau_\varphi$ simply coincides with the energy relaxation rate $1/\tau_\epsilon$. The latter (in metals, for reasonably low energies ω) is determined by inelastic collision between electrons (see Ref. 4 for review) and can be estimated as

$$\frac{1}{\tau_\varphi} \simeq \frac{1}{\tau_\epsilon} \sim \frac{1}{\nu_0 L_\omega^d} = \frac{\omega}{g(L_\omega)}, \quad (5.18)$$

where $L_\omega = \sqrt{D/\omega}$ is the length of diffusion in time ω^{-1} and $g(L) = \nu_0 D L^{d-2}$ is conductance of the d -dimensional sample with size L . For zero dimensional case the inelastic process of this type can be neglected completely since $\frac{1}{\tau_\varphi}$ compares with the level spacing only at the energies E^* of the order of the Thouless energy^{13,21}.

Using Eqs. (4.13) we can estimate dimensionless product $W_d \tau_\varphi$ as

$$\begin{aligned} W_d \tau_\varphi &\sim \left(\frac{\Delta}{\Omega} \right)^{\frac{2}{4-d}} g(\xi)^{\frac{2-d}{4-d}} \\ &\sim \left(\frac{\Delta}{\Omega} \right)^{\frac{2}{4-d}} \times \begin{cases} g^{1/3}(\xi) & d=1 \\ \log g(\xi) & d=2, \end{cases} \end{aligned} \quad (5.19)$$

where $\xi = L_\Delta$ is the coherence length. Since $\Delta \sim \Omega$, this estimation implies that as long as localization length L_{loc} exceeds ξ the width W_d is much bigger than $1/\tau_\varphi$ and inelastic collisions are irrelevant (L_{loc} can be estimated from the equation $g(L_{loc}) \sim 1$).

Together with Eqs. (2.13) and (3.43) for W_d and Eqs. (5.9)–(5.15) for Γ , Eq. (5.17) completely describes tunneling anomalies at $eV \sim \pm E^*$ for $W_d \geq T, \Gamma$ and $d = 0, 1$. For $d = 2$, Eq. (5.17) is valid only provided that the external magnetic field is parallel to the plane. The orbital effect of this perpendicular component on the tunneling anomaly is discussed in the next section.

D. Magnetic field perpendicular to the film

It was already mentioned that for zero- and one-dimensional cases orbital effects of magnetic field manifest themselves through addition $1/\tau_H$ from Eq. (5.12), to the parameter Γ , see Eqs. (5.6), (5.13), and (5.15). The same is true in two dimensions provided the magnetic field is parallel to the film plane⁴. However, effect of a component of magnetic field perpendicular to the plane requires a separate consideration.

Similarly to usual calculation of anomalous magnetoresistance^{22,4}, we need to derive and to solve equation for the Cooperon in perpendicular magnetic field rather than to take this field into account perturbatively. This equation is well known to be a Schrödinger equation in imaginary time for a particle with charge $2e$ and mass $1/(2D)$ in the magnetic field H . For $H = 0$ eigenfunctions of this equations are plane waves. When this field H is finite but parallel to the plane and weak enough (magnetic length $l_H = (\hbar c/eH)^{1/2}$ exceeds the film thickness a , or Ω_H , Eq. (5.13), is smaller than "perpendicular" Thouless energy $E_T = D/a^2$), it can be taken into account perturbatively. Eigenfunctions remain to be plane waves, so that Cooperon keeps its form Eq. (5.8), but the eigenvalues are shifted by τ_H^{-1} .

Contrarily, even weak perpendicular component of H changes eigenfunctions, and as a result the form of the Cooper pole is also modified. Each eigenfunction should be characterized by the number of Landau band n and by one of the components of momentum Q (one of the coordinates of the guiding center) rather than by both components of the momentum. Corresponding eigenvalue equals to $\Omega_H(n + 1/2)$, where Ω_H is given by Eq. (5.13), *i.e.*, it is determined by the number of Landau band, and it is independent of the location of the center.

As a result, in all previous calculations DQ_j^2 should be substituted by $\Omega_H(n + 1/2)$, and instead of integrating over (dQ_j), we have to sum over n and divide the result by $4\pi l_H^2$. At $H = 0$ integration over dQ is limited from above by

$DQ^2 \lesssim \Delta$, see discussion after Eq. (3.44). For the same reason we sum over n from 1 till $N \simeq \Delta/\Omega_H$. In order to evaluate $\delta\nu_\sigma(\omega)$, we have to perform calculation similar to that of Sec. III with such changes.

Equation (3.23) for the DoS should be rewritten as

$$\frac{\delta\nu_\sigma(\omega)}{\nu_0} = -\frac{\Delta^2}{\nu_0\Omega} \text{Im} \frac{\partial}{\partial\omega} \int_0^1 d\eta \frac{1}{4\pi l_H^2} \sum_{n=1}^N \gamma_\omega(\omega_{n\sigma}, n), \quad (5.20)$$

where $\sigma = \pm 1$ corresponds to \uparrow and \downarrow respectively, and the short hand notation

$$\omega_{n\sigma} = 2(\omega + \sigma E^*) + i\Omega_H \left(n + \frac{1}{2} \right), \quad (5.21)$$

is introduced. After obvious modification of Eq. (3.31), we obtain instead of Eq. (3.33)

$$\gamma_\omega(\zeta, n) = \frac{Z(\omega)}{-i\zeta + \Omega_H(n + \frac{1}{2}) + 2m(\omega)}, \quad (5.22)$$

where $Z(\omega)$ and $m(\omega)$ can still be expressed through β_0 and β_1 according to Eq. (3.34). Consequently, functions $\beta_0(\omega)$ and $\beta_1(\omega)$ can be connected with $\gamma_\omega(\zeta, n)$ by equations similar to Eq. (3.32):

$$\beta_p(\omega) = \eta \frac{\Delta}{\nu_0\Omega} \sum_{n=1}^N \frac{\gamma_\omega^2(\omega_n, n)}{[-i\omega_n + \Omega_H(n + \frac{1}{2})]^p}. \quad (5.23)$$

Equation (5.23) is valid for $p = 0, 1$ and for the both spin directions. We substitute Eq. (3.33) into Eqs. (5.20) and (5.23), carry out summation over n , and obtain Eqs. (3.41) and (3.43). The scale of the singularity coincides with W_2 from Eq. (3.43) while dimensionless function M_d is substituted by

$$M_H(x) = \ln \left(\frac{\Delta}{\Omega_H} \right) - \psi \left(\frac{1}{2} + \frac{x}{\alpha_H} \right). \quad (5.24)$$

Here, orbital effect of the magnetic field is characterized by dimensionless parameter $\alpha_H = \Omega_H/W_2$ and $\psi(x)$ is the digamma function

$$\psi(x) = \sum_{n=0}^{\infty} \left(\frac{1}{n+1} - \frac{1}{n+x} \right) - \mathbf{C},$$

and $\mathbf{C} \approx 0.577\dots$ is the Euler constant. If magnetic field is weak $\alpha_H \ll 1$, we can use the asymptotic expansion $\psi(x) \approx \ln x$, $x \gg 1$ and recover two-dimensional result M_2 from Eq. (3.44). Since function M_H depends on additional variable α_H only as on a parameter we can use the solution of Sec. III B to obtain density of states:

$$\frac{\nu_\sigma(\omega)}{\nu_0} = F_H \left(\frac{\omega - \sigma E^* + i\Gamma}{W_2} \right), \quad (5.25)$$

where energy scale W_2 is given by Eq. (3.43), we included previously discussed broadening mechanisms according to rule (5.5) with the rate Γ given by Eq. (5.15). Dimensionless function $F_H(x)$ is given by

$$F_H(x) = \text{Re} \frac{\alpha_H - \psi' \left[\frac{1}{2} + \frac{-ix+y(x)}{\alpha_H} \right]}{\alpha_H + \psi' \left[\frac{1}{2} + \frac{-ix+y(x)}{\alpha_H} \right]}, \quad (5.26)$$

where the function $y(x)$ is the solution of the equation

$$y(x) = \ln 4g - \ln \alpha_H - \psi \left(\frac{1}{2} + \frac{-ix+y(x)}{\alpha_H} \right).$$

The density of states in two dimensional films for different values of the parameter α_H is shown on Fig. 16.

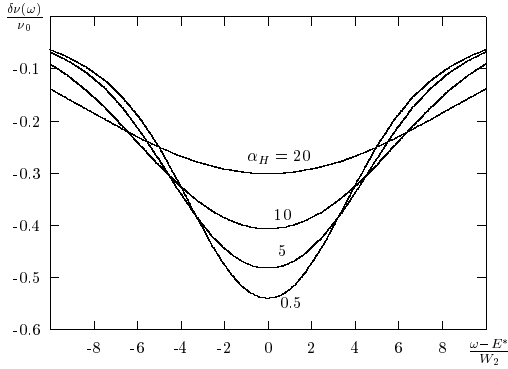


FIG. 16. Singularity in DoS of two dimensional films for spin-down polarized electrons for different values of dimensionless magnetic field $\alpha_H = \Omega_H/W_2$. Curves are plotted for conductance $g = 10$.

Closing this subsection, we present the asymptotic behavior of $F_H(x)$ for two limiting cases. In the weak fields $\alpha_H \ll 1$ the magnetic field slightly perturbs the two-dimensional result (3.53):

$$F_H(x) = F_2(x) + \frac{1}{12} \left(\frac{\Omega_H}{W_2} \right)^2 \text{Re} \frac{z^3(x)}{[1+z(x)]^2}, \quad (5.27)$$

where dimensionless functions $F_2(x)$ and $z(x)$ are defined in Eqs. (3.53) and (3.54) respectively.

In the opposite limit $\alpha_H \gg \max(1, \Gamma/W_2)$ the depth of the singularity is controlled by solely cyclotron frequency (5.13)

$$\frac{\nu_\sigma(\omega)}{\nu_0} = 1 - \begin{cases} \frac{W_2}{\Omega_H} \frac{\pi^2}{\cosh^2\left(\frac{\omega + \sigma E^*}{\Omega_H}\right)}, & |\omega + \sigma E^*| \lesssim \Omega_H; \\ 4\pi^2 \frac{W_2}{\Omega_H} \exp\left(-2\frac{\omega + \sigma E^*}{\Omega_H}\right) + \left(\frac{W_2}{\omega + \sigma E^*}\right)^2 \ln\left(\frac{\Omega}{\omega + \sigma E^*}\right)^2, & |\omega + \sigma E^*| \gg \Omega_H. \end{cases} \quad (5.28)$$

VI. EXPERIMENTS ON AL FILMS

The theoretical study presented in this paper was inspired by the experimental work of Wu, Williams, and Adams⁸. These authors studied tunneling anomalies in ultra-thin (about $4nm$ thick) *Al* films, which were driven into paramagnetic state by parallel magnetic field $H > H_{\parallel} \simeq 4.8T$. Both zero bias anomaly and anomalies at biases close to Zeeman splitting E_Z were observed. The authors attempted to fit the experimental results by the theory of Ref. 4, developed for normal metals and superconductors at $T > T_c$. The agreement appeared to be reasonable with one important exception: the positions of the satellite singularities E^{**} was lower in energies than that predicted by Ref. 4: experimentally it was fitted as

$$E^{**} \simeq E_Z - E_0; \quad E_0 = 0.17meV. \quad (6.1)$$

In our theory $eV_s = E^* < E_Z$, see Eq. (1.7), and the discrepancy is reduced even though it does not disappear. For instance, minimal value of E^* corresponds to the phase transition point $E_Z = \sqrt{2}\Delta$ and, according to Eq. (1.7), equals to $\Delta(\sqrt{2} + 1)/2 \simeq 0.47meV$, since $\Delta \simeq 0.39meV$. Experimental value $eV_s \simeq 0.38meV$ is about 20% (rather than 33% in comparison with Ref. 4) smaller. We do not have enough data to speculate about possible sources of this discrepancy. More experiments with serious quantitative analysis are needed to verify the present theory. Nevertheless, it may be worthwhile to briefly discuss here how the other experimental findings of Ref. 8 compare with the theoretical conclusions.

In Ref. 8, authors presented and discussed tunneling conductance $G(V, H)$ as a function of the bias voltage and magnetic field for two samples. Both samples were granular *Al* films about $4nm$ thick. Sheet resistance were different $R_{\square}^{(1)} \simeq 4.2K\Omega$, $R_{\square}^{(2)} \simeq 2.0K\Omega$. For both samples dips of the tunneling conductance at $V = \pm V_s$ were observed. The widths at half minimum (WHM) of these dips for both samples were about $0.15 \div 0.2meV$, while the depths were found to be quite different: $|\delta G/G|^{(1)} \simeq 0.12$ and $|\delta G/G|^{(2)} \simeq 0.05$.

One can interpret these experimental results in two different ways. The first interpretation is based on the assumption that the granular structure of the films is irrelevant, and they can be approximated as homogeneous 2D objects. Given the superconducting gap $\Delta \simeq 0.39meV$, Zeeman splitting $E_Z \simeq 0.57meV$ at magnetic field $H = 5T$, and R_{\square} , one can use Eq. (3.43) to determine W_2 : $W_2^{(1)} \simeq 0.03meV$; $W_2^{(2)} \simeq 0.015meV$. Since WHM of the anomaly should be compared with approximately $2W_2$, see Fig. 15c, we have not great but reasonable agreement, especially for the first sample. However the law $W_2 \propto \ln(g)/g$ from Eqs. (3.43) and (3.53) seems to contradict the experiment.

The alternative interpretation is based on the approximation of weakly connected *Al* grains: in the first approximation we neglect the coupling between the grains. This allows to use 0D expression for the width of the singularity W_0 , see Eq. (2.13). Given the electron concentration in *Al* $n = 1.8 \times 10^{23}cm^{-3}$ and their Fermi energy $E_F = 11.8eV$ ¹⁹, bare DoS estimates as $\nu \simeq 2 \times 10^{22}(eVcm^3)^{-1}$. Assuming that the grains in lateral directions have typical size $b \simeq 30nm$ ⁸, and that the film thickness is $a \simeq 4nm$, we can estimate the mean level spacing $\bar{\delta} \simeq 1/(ab^2\nu) \simeq 0.03meV$. Substitution of this value of $\bar{\delta}$ into Eq. (2.13) gives $W_0 \simeq 0.11meV$. This is in a good agreement with the experiment, since WHM at zero dimensions according to Fig. 15a should be compared with $2W_0 \simeq 0.22$.

In order to understand the substantial difference in amplitudes of the tunneling anomalies for the two samples, let us discuss the effect of coupling between the grains. This coupling results in a finite dwell time τ_{dwell} which an electron spends in a given grain before tunneling into a neighboring one. We can determine τ_{dwell} from D -the constant of the diffusion at times bigger than τ_{dwell} using the relation $D \simeq b^2/(2\tau_{dwell})$. Given the sheet resistance $R_{\square}^{(1,2)}$, DoS ν , and the film thickness a , one can estimate D as $D^{(1)} \simeq 0.2cm^2/sec$, $D^{(2)} \simeq 0.4cm^2/sec$. As a result

$$\frac{\hbar}{\tau_{dwell}^{(1)}} \simeq 0.05meV \quad \frac{\hbar}{\tau_{dwell}^{(2)}} \simeq 0.1meV.$$

Now we can explain the difference in the depths of the anomalies in the two samples assuming that \hbar/τ_d contributes to Γ from Eq. (5.15). One can see from Fig. 15a that the dip at $\Gamma = W_0/2$ is approximately twice as deep as the one at $\Gamma = W_0$. At the same time, WHMs in these two cases are close to each other.

Note that Eq. (5.7) with $\Gamma = \hbar/\tau_{dwell}$ can be justified only for $\tau_{dwell}W_d > \hbar$. Theoretical investigation of the crossover between 0D and 2D behavior in granular films goes beyond the framework of this paper, though such a study can be important for a quantitative discussion of experiments.

From the perpendicular critical field $H_{c\perp} \simeq 1.5T$ and the dimensions of a grain one can estimate $1/\tau_H$ and find that it is irrelevant for the experiment⁸. The same is correct for spin-orbit scattering. Recent studies of tunneling through *Al* grains⁹ show that the difference of the g -factor from 2 is very small not only in average, but also for a given orbital as well. Both \hbar/τ_H and \hbar/τ_{so} are probably smaller than $0.01meV$ and much smaller than \hbar/τ_{dwell} .

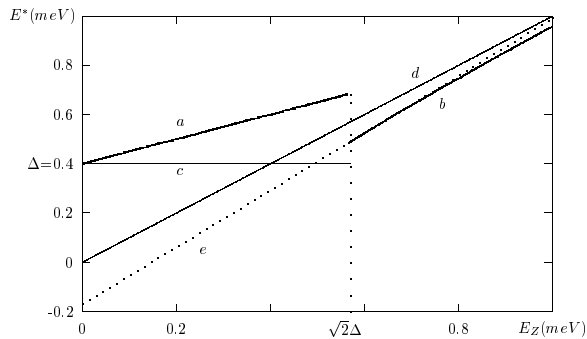


FIG. 17. Position of the minimum in the DoS as the function of the Zeeman splitting E_Z for $\Delta \simeq 0.4meV$: (a) Theoretical prediction for the superconducting state⁵, see Fig. 1a; (b) Our theoretical prediction, Eq. (1.7) for the paramagnetic state; (c) Half distance between maxima in the DoS in the superconducting state; (d) $E^* = E_Z$ law predicted for the normal metal⁴; (e) Approximation of Eq. (1.7) by a straight line.

Let us now return to the discussion of the dip location. Note that a dip of DoS at finite bias exist in both superconducting and paramagnetic states. According to idealized Fig. 1a in superconducting side of the Clogston-Chandrasekhar phase transition this anomaly is located at $eV = \Delta + E_Z/2$ (line “a” in Fig. 17). However, probably

due to the smearing of the DoS singularities, experimentally the minimum was found in the middle between two peaks in the DoS, *i.e.* at $eV \simeq \Delta$ (line “c” at Fig. 17). As it was already mentioned, the experimentally found position of the singularity is lower than our theoretical prediction (1.7). In fact there were no jump in E^* observed at the point of the first order phase transition. This discrepancy may be due to the inhomogeneous broadening of the transition-different granulars may have slightly different Δ . Another possibility is illustrated on Fig. 17. In the interval of magnetic fields where the measurements were done the theoretical dependence Eq. (1.7) (line “b” at Fig. 17) can be approximated by

$$E^* \approx rE_Z - 0.17meV \quad (6.2)$$

with numerical factor $r \simeq 1.15$ is slightly larger than 1 (line “e” at Fig. 17). Comparing Eq. (6.2) with the experimental fit (6.1), we see that the theory would agree with experiment very well if we assume that actual g -factor is smaller than its bare value, *i.e.* $g_L = 2/r \approx 1.72$.

VII. CONCLUSION

This paper is devoted to the anomalies of the tunneling density of states of low dimensional ($d = 0, 1, 2$) superconductors in external magnetic field. We concentrated on the Clogston - Chandrasekhar (CC) phase transition, *i.e.* the destruction of the superconductivity by the magnetic field by virtue of the Zeeman splitting. As a result normal paramagnetic state of electrons is formed.

The main conclusion we can draw from our study of CC state is, that despite this state being normal (mean-field superconducting order parameter vanishes), it is drastically different from a usual normal metal with some attractive interaction. The latter state appears, *e.g.*, in a superconductor at temperatures higher than the transition temperature T_c . The difference becomes apparent when one studies excited states rather than those closed to the ground state.

Superconducting fluctuations in a usual normal disordered metal were known to contribute to the zero-bias tunneling anomaly as well as to Zeeman anomalies at the bias eV equal to Zeeman splitting⁴. However, these contributions (effects of the interaction in Cooper channel) are similar or weaker than effects of Coulomb repulsion of electrons, unless the system is anomalously close to the transition, *i.e.* it is not in Levanyuk-Ginzburg region. This means that the effects of superconducting fluctuations can be taken into account perturbatively almost everywhere, (except the very vicinity of the transition temperature) if the system is not too dirty. The perturbative approach (expansion in inverse powers of the conductance g) is valid as long as all of the characteristic length scales involved into the problem do not exceed the localization length L_{loc} .

Tunneling anomalies in CC normal state studied by us are quite different. First of all, its position $eV = E^*$, see Eq. (1.7), is different from the Zeeman splitting E_Z . However, what is more important, the perturbative corrections to the density of states $\nu(\omega)$ are much singular at ω close to E^* than the same order in g^{-1} corrections in usual normal metals. Because of this, the perturbative approach fails at parametrically wider energy interval $|eV - E^*| \leq W_d$ around the singular bias than that for the normal metal. Using Eqs. (3.43), one can check that the length scale L_W which corresponds to W_d is much less than $L_{loc}^{(d)}$, provided L_{loc} exceeds superconducting coherence length ξ . Indeed, since the localization length can be estimated as $L_{loc}^{(1)} \simeq D\nu^{(1)}$ and $L_{loc}^{(2)} \simeq l \exp(D\nu^{(2)})$, (where l is the mean free path, D is the diffusion coefficient, and $\nu^{(d)}$ is d -dimensional DoS) the characteristic spatial scale corresponding to the singularity, L_{W_d} , can be written as

$$\frac{L_{W_1}}{L_{loc}^{(1)}} \simeq \left(\frac{\xi}{L_{loc}^{(1)}} \right)^{2/3}$$

$$\frac{L_{W_2}}{L_{loc}^{(2)}} \simeq \frac{\xi}{L_{loc}^{(2)}} \sqrt{\ln \left(\frac{L_{loc}}{l} \right)}.$$

The fact that $W_d \gg D/L_{loc}^2$ makes it necessary and also possible to go beyond the perturbation theory – one has to sum only most diverging terms, and it is allowed to neglect usual weak localization and interaction corrections. It turns out to be possible to sum directly whole series of the perturbation theory and thus determine the shapes of the singularities at all dimensions.

The singularities are characterized by their widths W_d given by Eqs. (2.13) and (3.43). For zero dimensional grains our theory predicts a hard gap in the density of states with a given spin direction, centered at $\omega = E^*$. For one dimensional wire the shape becomes universal (independent on $\nu^{(1)}$ and D) when energy is measured in units of W_1 , see Eq. (3.52). It means that the depth of the anomaly is universal. In the case of two dimensional film the depths of the anomaly is not universal and behaves as the inverse logarithm of the conductance, see Eq. (3.53).

The reason for the effects of superconducting fluctuations in CC metal to be dramatically enhanced in comparison with the usual case is the presence the pole-like singularity in the correlation function of these fluctuations. This pole at a finite frequency appears due to the fact that CC transition is of the first order. Contrarily, the temperature driven transition from superconductor to normal metal is of the second order, and in a usual normal state the correlator of the superconducting fluctuations is a smooth function of the frequency, *i.e.* any superconducting excitation decay very rapidly. We believe that the strong anomalies of the excitation spectrum at finite energies is a generic feature of any state created as a result of a first order quantum phase transition.

ACKNOWLEDGMENTS

Discussions with A.I. Larkin and B.Z. Spivak are acknowledged with gratitude.

-
- ¹ M. Tinkham, *Introduction to superconductivity*, (McGraw-Hill, New York, 1980).
² A.M. Clogston, Phys. Rev. Lett. **9**, 266 (1962); B.S. Chandrasekhar, Appl. Phys. Lett. **1**, 7 (1962).
³ I. Giaever, Phys. Rev. Lett., **5**, 464 (1960).
⁴ B.L. Altshuler and A.G. Aronov, in *Electron-Electron Interaction in Disordered Systems*, edited by A.L. Efros and M. Pollak (North-Holland, Amsterdam, 1985).
⁵ P. Fulde, Adv. in Phys. **22**, 667 (1973).
⁶ I.L. Aleiner and B.L. Altshuler, Phys. Rev. Lett. **79**, 4242 (1997).
⁷ A.A. Abrikosov, L.P. Gorkov, and I.E. Dzyaloshinskii, *Methods of Quantum Field Theory in Statistical Physics*. (Prentice-Hall, Englewood Cliffs, NJ, 1963).
⁸ W. Wu, J. Williams, and P.W. Adams, Phys. Rev. Lett. **77**, 1139 (1996).
⁹ C.T. Black, D.C. Ralph and M. Tinkham, Phys. Rev. Lett. **76**, 688 (1996).
¹⁰ F. Braun, J. von Delft, D. C. Ralph, and M. Tinkham, Phys. Rev. Lett. **79**, 921 (1997).
¹¹ For review see *e.g.* D.V. Averin and K.K. Likharev in *Mesoscopic phenomena in solids*, edited by B.L. Altshuler, P.A. Lee, and R.A. Webb (North Holland, New York, 1991).
¹² Ya.M. Blanter, Phys. Rev. B **54**, 12807 (1996); O. Agam, N.S. Wingreen, B.L. Altshuler, D.C. Ralph, and M. Tinkham *ibid.*, **78**, 1956 (1997); Ya.M. Blanter and A.D. Mirlin, Phys. Rev. E **55**, 6514 (1997).
¹³ B.L. Altshuler, Y. Gefen, A. Kamenev, L.S. Levitov, Phys. Rev. Lett. **78**, 2803 (1997).
¹⁴ S. Hikami, Phys. Rev. B, **24**, 2671 (1981).
¹⁵ Numerical coefficient in the formula for W_1 is different from that in Ref. 6 because of the algebraic error in this reference.
¹⁶ L.N. Cooper, Phys. Rev. **104**, 1189 (1956).
¹⁷ H.A. Kramers, Proc. Amst. Acad. **33**, 959 (1930).
¹⁸ V.E. Kravtsov and M.R. Zirnbauer, Phys. Rev. B **46**, 4332 (1992).
¹⁹ N.W. Ashcroft and N.D Mermin, *Solid State Physics*, (Holt, Rinehart and Winston, New York, 1976).
²⁰ S. Hikami, A.I. Larkin and Y. Nagaoka, Progr. Theor. Phys. **63**, 707 (1980).
²¹ U. Sivan, Y. Imry and A. Aronov, Europhys. Lett. **28**, 115 (1994).
²² P.A. Lee and T.V. Ramakrishnan, Rev. Mod. Phys. **57**, 287 (1985).